UNIVERSIDAD NACIONAL AUTÓNOMA DE MÉXICO

Master's Program in Science and Materials Engineering

Centro de Física Aplicada y Tecnología Avanzada

"Development of flexible soft ionic materials based on deep eutectic systems and biopolymers"

A THESIS

In Partial Fulfillment of the Requirement for the Degree of

MSc in Materials Science and Engineering

P R E S E N T S

Saúl Carrasco Saavedra

MAIN TUTOR

Dr. Josué David Mota Morales
Centro de Física Aplicada y Tecnología Avanzada

TUTOR COMMITTEE

Dr. Gonzalo Ramírez García
Centro de Física Aplicada y Tecnología Avanzada
Dr. Eden Morales Narváez
Centro de Investigaciones en Óptica A.C.

Santiago de Querétaro, Qro. 08/06/2023

Universidad Nacional Autónoma de México
UNAM
Biblioteca Central
Dirección General de Bibliotecas de la UNAM

UNAM – Dirección General de Bibliotecas
Tesis Digitales
Restricciones de uso

DERECHOS RESERVADOS ©
PROHIBIDA SU REPRODUCCIÓN TOTAL O PARCIAL

Todo el material contenido en esta tesis esta protegido por la Ley Federal del Derecho de Autor (LFDA) de los Estados Unidos Mexicanos (México).

El uso de imágenes, fragmentos de videos, y demás material que sea objeto de protección de los derechos de autor, será exclusivamente para fines educativos e informativos y deberá citar la fuente donde la obtuvo mencionando el autor o autores. Cualquier uso distinto como el lucro, reproducción, edición o modificación, será perseguido y sancionado por el respectivo titular de los Derechos de Autor.

Index

Technical acknowledgments

I would like to express my deepest appreciation for the generous scholarship that I have been awarded by CONACYT for the past two years. It is with immense gratitude that I acknowledge the invaluable support you have provided me in pursuing my academic and research endeavors. Also, I want to thank for the grant of PAPIIT No. IA206022 for which I got the support for my project.

I want to thank the "Laboratorio Nacional de Caracterización de Materiales" of CFATA UNAM, especially Dr. Beatriz Millán Malo for her support with X-ray diffraction characterizations, and M.I. Gerardo Fonseca for his support with the mechanical essays on my materials. I would also like to thank Dr. Mario Enrique Rodríguez García for allowing me to use his equipment to characterize my materials through FTIR. Similarly, I am grateful to Dr. Luz María López Marin and the "Nanobio-óptica" Lab for the use of their UV-Vis spectrophotometer. I also thank Dr. Reinher Pimentel for his guidance in mold preparation as well as designing and conducting various optical experiments.

Also, thanks to the University of Guanajuato and particularly to the Department of Chemistry and their technical manager Karla Alejandra Barrera Rivera, for their assistance in obtaining the DSC thermograms.

I would like to extend my sincere gratitude to Tufts University, particularly Professor Matthew Panzer, who kindly accepted me for a short-term visit at the university. His assistance with the electrical and mechanical characterization of my materials was invaluable.

Personal acknowledgments

I want to extend special thanks to Kaori and her family, Dr. Rodrigo Carrillo, and Ms. Beatriz Sanchez for welcoming me into their home during my stay in Boston, for their unconditional support, and the wonderful experience I had while being with them. I will never forget this tremendous support.

I want to say thank you to my tutor committee, Dr. Gonzalo Ramírez and Dr. Eden Morales for all the support given in the last two years. Your deep knowledge and your expertise have been an inspiration for the improvement of my work and my growth as a future researcher. To my lab group and friends in the Polymer Lab and the CFATA campus, thank you for all your support in all different ways, our time together during the courses, talks, or lunch time has made my time enjoyable.

Also, I would like to express my sincere gratitude to Dr. Josué for your guidance and mentorship during my studies. Your unwavering support and expertise have been instrumental in shaping my academic and professional journey. I am truly grateful for your valuable insights, encouragement, and dedication to my success. Thank you for being an exceptional advisor.

Last but not least, to my family, my parents, and my brother Emilio, who have been unwavering support that has brought me this far and I am confident will take me even further. To all my friends but specially Rubén and Andrea, who have been indispensable in my life for many years, thank you.

Abstract

Due to their low cost, stability, environmental friendliness, high conductivity, non-volatility, high stability and easy preparation, deep eutectic solvents have been used as green electrolytes fot the design of new soft materials. Gelatin-based eutectogels have been previously proposed as skin-like soft materials sensors due to the remarkable combined properties of their components: a natural self-assembling capacity of denatured collagen chains and the low-volatility and ionic conductivity of the nonaqueous deep eutectic solvent electrolyte, that overall result in soft materials with high stretchability. In the search for expanding the properties of these biobased stretchable materials, this thesis introduces a natural nanomaterial -cellulose nanocrystals, CNCs- as a reinforcement to the polymer matrix to boost their mechanical performance. Herein we report two different eutectogels containing 1.0 wt% of CNCs surface-functionalized with -OSO_3H and COOH groups. After the nanocrystal's incorporation into the eutectogels, the resulting materials increased the stretchability (up to ~375%) and an ionic conductivity of 3.0 $mS\ cm^{-1}$ at room temperature was observed. Additionally, the possible arrangement of CNCs within the eutectogel generated new optical effects like birefringence and shear-induced birefringence visible under polarized light, which allow the material to have an optical response based on mechanical deformation. Thus, the novel properties conferred to the all-natural gelatin-based eutectogels by CNC incorporation can further extend the eutectogel's applications towards new areas in biocompatible soft materials, sensors, and substrates for soft robotics, without sacrificing the overall degradability and sustainability.

Key words: **biopolymers, gelatin, deep eutectic solvents, soft materials, cellulose nanocrystals.**

Figure Index

1. Introduction

Due to the arrival of new technologies that make our lives easier, like wearable devices, smartphones and flexible screens, the interest for the development of new flexible electronic devices has aroused significant attention. However, the one-use and disposal culture shown by the human being has caused an increment in the e-waste produced in a global scale, where the accumulation of contaminant and non-recyclable materials has become a major problem in the world.

The above mentioned hast set a new direction towards the design of flexible electronics, where the use of greener materials and processes must be followed to fulfill the high demand of sensors, actuators, and other flexible devices in a sustainable and responsible way. Commonly, in gel form, *soft materials* are chosen as substrate for this type of applications because of its resemblance with biological tissues, degradability, flexibility, and biocompatibility. Formed by a solvent and a gellant, gels are three-dimensional networks assembled of macromolecules or aggregates capable of retaining significant quantities of solvent. As water is the universal solvent, *hydrogels* represent sustainable, eco-friendly, low cost and biocompatible materials with remarkable mechanical properties. Unfortunately, hydrogels are susceptible to solidify at freezing temperatures and their volatility in the environment limits their long-term stability.

A common approach to surpass their flaws, is the solvent substitution for those capable of improving the physicochemical properties of the gels. Ionic liquids (IL) represent a solvent alternative for the preparation of soft materials, their low volatility overcomes the high volatility in the hydrogels and provides ionic mobility in the system, which imparts an ionic character to the gels. Nonetheless, the use of IL has notably been reduced due its possible toxicity and high production cost. Deep eutectic solvents (DES), however, are presented as a new class of *green design solvents* whit the potential to replace the conventional ionic liquids. Briefly, the DES of interest in this research are formed by the mixture of a quaternary ammonium salt with a hydrogen bond donor (commonly amides, carboxylic acids or polyols) in a certain molar proportion. Besides having similar properties to ionic liquids (high thermal stability and ionic conductivity) DES's immense potential relies on its easy preparation, low toxicity, possible biodegradability, low cost, and scalability.

In combination with a gellant agent such as biopolymers, *eutectogels* are novel three-dimensional structures with an ionic character capable of operating in a broader range of temperatures as well as extreme environmental conditions such as vacuum. Also, as all those

biopolymers come from natural sources, a priori they grant the materials with a biodegradable nature, also they offer a self-assembling ability which avoids the use of any external crosslinker agent.

Gelatin, for instance, is a byproduct obtained from the hydrolysis of collagen and is a renewable resource. Owing to its natural properties such as reversible sol-gel transition, permeability, semi-solid behavior and, the ability to form H bonds and electrostatic interactions, gelatin has been widely used as a building block for the design of soft materials. It is also naturally compatible with ionic liquids and, therefore, with deep eutectic solvents. In the literature, the use of gelatin in DES has been previously reported by the Panzer group who previously designed a non-volatile gelatin-based pressure sensor, which also exhibited a transparent character along with a noticeable conductivity (2.5 $mS\ cm^{-1}$) and a high stretchability ($\sim 300\%$), confirming that gelatin is a good gellant agent for the design of green eutectogels.

While all those properties are useful and have a high potential in flexible electronics, the fact is that those materials can still be optimized, and new properties can be explored through different approaches. Used for physical crosslinking and mechanical reinforcement in soft materials, cellulose nanocrystals (CNCs) are cellulose crystalline regions in the form of rods that have been employed as organic-mechanical load to improve thermal and mechanical properties for some biocomposites due to its high thermal stability, great mechanical performance, and another interesting property that can be conferred to the material in which they are integrated such as shear birefringence, self-healing and much more.. Also, regarding nanomaterials, the surface chemistry is a particularly important issue that must be taken in consideration. Typically, because of its acid extraction treatments, a high number of sulfate groups are normally found in this type of nanomaterials and certainly limit the number of non-covalent interactions that the cellulose can achieve. Looking then for a better interaction between the cellulose, the gelatin, and the DES, CNC's surface can be modified by substituting sulfate groups for a more hydrophilic ones, like -OH groups found in carboxylic acids which not only facilitate the cellulose dissolution in a polar solvent, but also promote the formation of new non-covalent interactions along the eutectogel which are reflected in a boost in the material's different properties and overall performance.

In the present work, we present the design, characterization and the proposal of a strain-sensor of a gelatin based eutectogel containing nonaqueous choline chloride-ethylene glycol deep eutectic solvent (1:2 molar) reinforced with commercial and functionalized CNC in different proportions, sulfated and carboxylated CNC, respectively

2. Background

2.1 Flexible electronics

Considering that cables and wires are the simplest example of flexibility, it is likely that the definition of flexible electronics had suffered modifications along the years. The recent growth in materials science has resulted in the development of nanomaterials, conductive polymers, organic semiconductors and amorphous silicon that, along with a variety of unconventional materials, have marked the way electronic devices are made. [1]

Flexible electronics is described as electronic circuits that can bend and stretch, promoting noticeable versatility in different applications and a low-cost manufacturing process. [2] Due to the high economic impact that conventional electronics represent, there is an important technological jump that flexible devices are meant to be. Even though the concept of flexible electronics has been around since the 60's, over the last two decades there has been an increase in the interest, commercialization, and investment in this kind of technologies. Just to mention an example, companies like Royole, Huawei and Samsung begun the release of flexible screen mobile phones back in 2018, [3] whereas it is expected that the market of flexible electronics grows from $41.2 Billion (2020) to $74 Billion by 2030. [4]

Flexible electronics has found a niche of opportunities both in industry and academics (Figure 1) in the areas of wearable devices, screen design, robotic skins, photovoltaics, energy harvesting and sensing. [5] These curvilinear surfaces have aroused interest because of its innovative applications potential. While traditional electronics have already been used for these functions, it is expected that flexible electronics boost the performance and changes the way conventional technologies are designed.

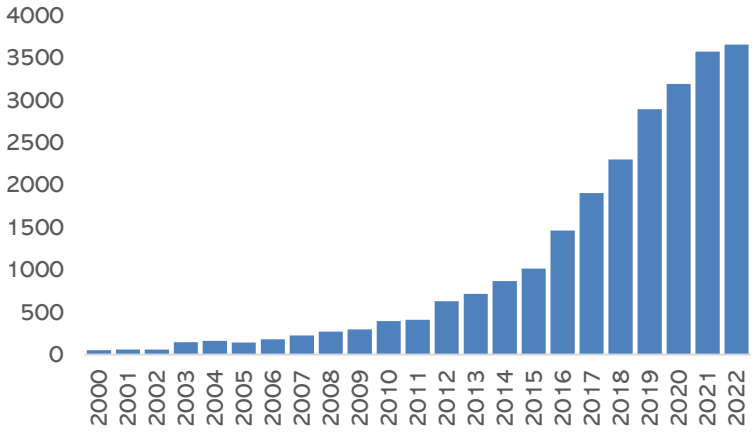

Figure 1. Web of Science research publications pear year obtained from the term "Flexible Electronics".

Typically, a flexible electronic device is built by the next key components: substrate, active layer (or functional layer), and the interface layer. The active layer includes the electric components, such as electrical circuits. The interface keeps the active layer on or inside the substrate, whereas the substrate is the base to build up devices. [6] The unconventional morphologies as well as the robust requirements for the correct functioning of flexible devices makes flexibility, elasticity, and toughness a requisite for any desired material for this kind of applications. By extent, a desired functional material for flexible electronics should be designed with an excellent mechanical deformability being capable of bending, rolling, folding and stretching, besides specific functions desired for certain application, e.g. optoelectronic response or stimuli responsive behaviors. [1]

Figure 2. Flexible electronics applications may include flexible screens, photovoltaics, wearable devices, soft robotics and flexible circuits and PCB. Image by author.

The main function of the substrate is to support and protect devices on it. In the polymers area, many commercial polymers have been used as flexible substrates, including polyvinyl alcohol (PVA), Polyethylene terephthalate (PET), Polyamide (PI), polyethylene, polyurethane (PU), polydimethylsiloxane (PDMS), etc. PI, for example, has an outstanding heat and corrosion resistance, as well as a noticeable mechanical flexibility. PDMS is similar in mechanical properties and is facile to prepare. The low-cost effective and pleasurable light penetration makes PET an efficient substrate for conductive substrates. [7]

It is relevant to mention that as we live in a technological era, the disposal of smart devices has become a matter of concern, as the way we use and dispose of technology results in a negative environmental impact shown by the growing electronic waste. [8] Discounting the amazing properties of the materials above, the increase in e-waste (more than 90% for substrate) has settled the direction in the look for eco-friendly and biodegradable substrate materials with outstanding flexibility and low cost [9]. There is no surprise that the design of flexible electronic devices veers to a sustainable strategy along with bioinspired and biomimetic design approaches. The use of natural building blocks and raw materials is preferred by their low-cost, large-scale availability, and potential biodegradability and biocompatibility, all hallmarks of green and sustainable materials. Thus, these raw natural materials not only reduce the production costs of the devices but also allow the easy disposition of the devices once accomplished their lifespan. [10]

2.2 Soft Materials

Catalogued in 2000 by *Science* as one of the top ten scientific and technological achievements [11], the flexible electronics science is a high multi-disciplinary discipline which supports from physics, chemistry, materials science, electronics and mechanical and electrical engineering in order to further develop the exceptional characteristics for each component of electronic devices. One big approach to design these new devices is to employ intrinsically *soft materials* as building blocks, such as small molecules and polymers [7] aided by nanomaterials.

The soft-matter approach focuses primarily on soft materials and fluids developed through polymer chemistry, condensed soft-matter physics, soft lithography, and soft microfluidics. Because of the vast list of materials included in the definition, authors like Majidi define a soft material as "*any fluid, gel, or material with a shear modulus less than 10 MPa"*. [12] Another significant definition is *"materials that exhibit low stiffness or low resistance to deformation under an applied load, they have a low elastic modulus and are easy to deform."* [13] In contrast to conventional rigid materials, soft materials merge from a bioinspired approach where natural organisms are the perfect example of composites that serve as starting point to further designing high performing functional materials with a unforeseen flexibility, deformability, and shape manipulation.

Common examples of soft materials include elastomers (like rubber) and gels. Elastomers have modulus between 0.1 and 10 MPa and, in general, they are elastic materials with a high stretchability and elastic resilience. PDMS is a commonly used elastomer for soft microfluidics and soft robotics due to their low modulus, high strain limit and low hysteresis between loading and

unloading cycles. [12] On the contrary, gels combine the properties of soft polymers and fluids, they can be infused with a variety of different fluids like water or organic solvents. Their solid phase exhibit elastic properties and the possibility of handling mechanical deformations. Gels may have a synthetic origin (polyethylene oxide, PVA) or naturally derived polymers like agarose, alginates, collagen, or cellulose biopolymers. [14]

With a tremendous possibility of designing soft materials, they have been foresighted as a promising technology to be developed in the next decades. According to a publication in *Science Robotics* [15], a research conducted in *Web* of *Science* from 2010 to 2020 about the most highly cited papers on medical robots describes a tremendous increase in the number of publications about *soft robotics, wearable robots, capsule robots,* and some other hot topics involving medical applications. Even if soft materials are not mentioned in Figure 3 as such, the parallel research and discovery of brand-new soft materials is certainly implied, increasing the interest on fabricating these technologies.

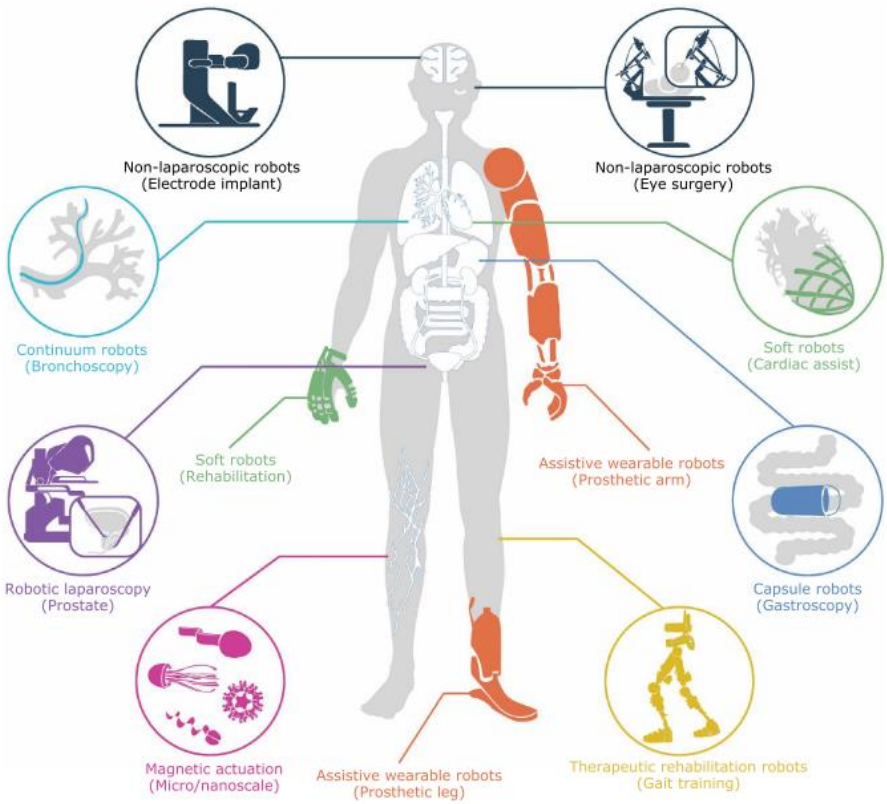

Figure 3. Example clinical applications for the hot topics of the decade. Recovered from: *Sci. Robot.*, vol. 6, no. 60, 202

2.2.1 Gels

Despite existing a plethora of soft materials used for nonconventional electronics (elastomers, interpenetrated polymer networks, block polymers, etc.) gels are the most used materials for this type of applications. Not being considered completely a solid nor a liquid, gels are semisolid systems where the predominant phase is a liquid and the second component acts as a gelator which triggers the formation of a three-dimensional network. [16] These semisolid structures may have properties ranging from soft and weak to hard and tough; they can be classified based on their liquid phase, wherein the most common gels are the *hydrogels*.

2.2.1.1 Hydrogels

Hydrogels are soft, deformable, transparent materials; they are highly hydrophilic, and, because of the hydrophilic character of the network, they can retain a high-water content which provides them a biocompatible nature. Also, his high degree of water confers a prominent level of transparency to the material, making it suitable for optical applications, moreover, the mobility of the ions in the liquid phase allows the hydrogel to perform as an ionic conductor reaching a conductivity up to $\sim 10\, S\, cm^{-1}$ (depending on the presence of electrolytes within the gel) and an elastic modulus typically in the range of 1-100 kPa. [17] The low cost of the solvent as well as their easy preparation and biocompatible character makes hydrogels as predominant materials in the scientific literature among all other electrolyte materials. A research conducted in the Web of Science database in late April 2022 for the topic “hydrogel”, yielded over 35000 documents published just in the last 5 years. [18]

Because of its easy preparation and broad applications in fields such as biomedical engineering, hydrogels have been discussed as a separate class of materials. [19] Hydrogels can be shaped into different forms based on the desired application, such as coatings, membranes, patches, wound dressings, solid forms like soft contact lenses or to encapsulate drugs or capsules for oral ingestion. [20] The versatility of hydrogels concerns to soft materials and flexible electronics, since they can respond to diverse external stimuli via interactions between the polymer network and water hydrogels have been proposed as magnetic actuators, temperature sensors, soft chemical sensors, stress/strain sensors etc (Figure 4. Features of hydrogels and soft robots. Materials Today Physics, Volume 15, 2020, 100258.Figure 4). [21] For instance, Guo et al. proposed the design of a double stimuli poly(acrylamide-co-maleic anhydride) soft hydrogel with a high stretchability, tensile strength and toughness, where the volatility of the gel was an important

issue. [22] Lin and coworkers developed a stretchable hydrogel which can be used as a compliant circuit bord, yet, the material has a low modulus of just 10 kPa. [23]

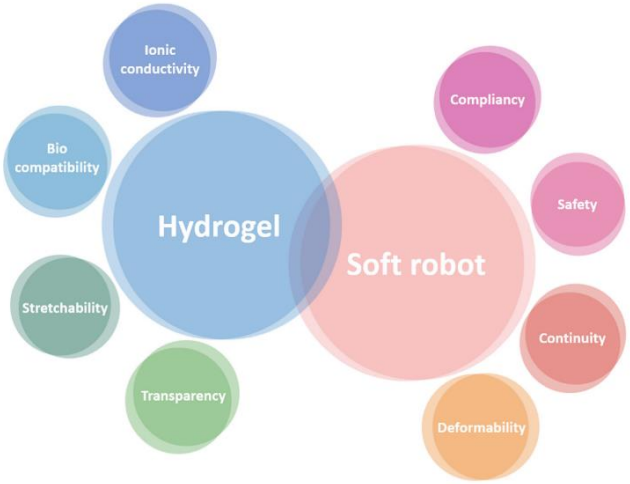

Figure 4. Features of hydrogels and soft robots. Materials Today Physics, Volume 15, 2020, 100258.

Nevertheless, many hydrogels have flaws concerning desired properties for flexible devices such as flexibility and toughness. Their lack of mechanical toughness and stretchability is then a huge limitation for their continuous use where they short life span plays against their robust operation on a daily basis. [19] It's also inevitably that conventional hydrogels are affected by freezing temperatures and suffer from evaporation at higher temperatures, causing a decrease and loss in volume, conductivity, durability, and flexibility, which consequently restricts the applications of this materials in the long-term and under harsh environments. Also, their low sensing sensibility, narrow detection range, easy damage, instability under extreme conditions, non-degradability and poor adhesion significantly hindered their application in flexible electronics. [24] There exists then an urgent need to replace the aqueous solvent for gel-based materials aiming for nonvolatility, long-lasting moisture, and long-term stability qualities.

2.2.2 Ionogels

On the contrary, ionogels are soft materials whose liquid phase is composed by an ionic liquid (IL) and a gelator. Since their pioneering discovery, ionic liquids have emerged as a new class of promising solvents, sometimes referred to as low melting point salts (below 100 °C) whose melts are composed of discrete ions. [25] ILs offer the chance to chemically modify the cationic structure in combination with a large number of anions, so, a broad range of ILs with different properties can exist, where noticeable changes in different physical properties such as melting

point, solubility, viscosity, density, conductivity and refractivity (among others) are unique for each pair of counterions. [26] Also, ILs present almost negligible vapor pressure, high thermal stability and low flammability, for which have been proposed to overcome hydrogel's limitations, including additional conductivity properties.

When an IL is mixed with a gelator an ionogel is formed. Ionogels are IL-based composites that typically consist of an IL and solid 3D networks. These materials share some similarities to hydrogels since they are ionic in nature, [16] however, ILs do not evaporate at high temperatures neither crystallize at low temperatures, therefore exhibiting a higher temperature stability, also, because of its ionic nature, the conductivity in this semi-solids is noticeable high without the addition of an extra component. [3] Having all these novel properties, ionogels have found a huge niche of applications in electrochemistry, bioelectronics and environmental science, just to mention some of them.

In previous years, soft ionic materials based on ILs have attracted attention to develop flexible and stretchable materials. For instance, Tamate et al. designed a self-healing diblock polymer with dimethylacrylamide (DMAA) and acrylic acid a (trifluoromethylsulfonyl)imide(TFSI) IL, where the hydrogel exhibited a maximum tensile strength, elongation at break and conductivity of 320 kPa, 12 $mS\ cm^{-1}$ and 400%, respectively. [27] Gu and collaborators successfully prepared an ionogel using a triblock polymer of styrene-*b*-ethylene oxide-*b*-styrene through self-assembly with a conductivity of 10 $mS\ cm^{-1}$ and an elongation at break of 350%. Zhu et al. exploited the IL's ability to disperse nanomaterials and introduced cellulose nanocrystals (CNCs) and graphene oxide (GO) into a polyvinyl alcohol (PVA), polyacrylic acid (PAA), and polyacrylamide (PAM) triple network ionogel, where a maximum tensile strength of 15.9 MPa and a tensile elongation at break of 610% were obtained.

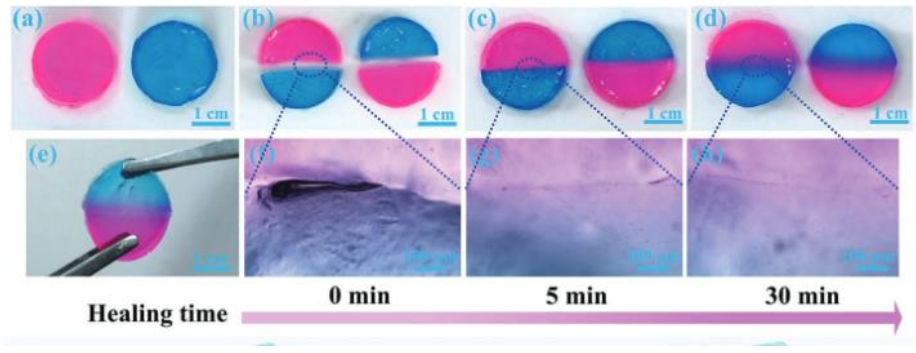

Figure 5. Self-healing is a property achievable in ionic liquids-based gels. Adv. Funct. Mater. 2022, 32, 2204565.

The ever-increasing bibliography about soft materials and ILs have gathered examples on how their coupling is a promising strategy for stretchable and conductive materials production. In the same line, serious back draws have been identified such as the issue of IL's toxicity, poor degradability, and certain unfavorable physical properties, such as high viscosity or high-cost production. [28] It is worthy to mention that the scope not only of this project but also the author's, is towards a sustainable, green and environmentally friendly direction towards the 12 principles of green chemistry. Following the last statement, it has been reported that deep eutectic solvents (DESs) are emerging as an alternative for not only replacing hydrogels but also ILs because of its similar features. Briefly, type III deep eutectic solvents (DESs) are low transition temperature mixtures mainly constituted by ions and non-charged molecules [29] whose main components are mainly non-toxic, cheaper, and biodegradable, giving the DES an outstanding greener character as well as a safer option to work than ILs.

The potential to scale-up the DESs preparation and implementation as well as their easy preparation has led to the design of brand-new novel materials known as *eutectogels,* which share similar properties to ionogels but without the drawbacks that ILs present. Nonetheless, DESs as well as the eutectogels will be discussed in the next sections of this project.

Figure 6. 12 principles of green chemistry. Recovered from "Designing & Facilitating a Bioeconomy in the Capital Regional District Learning Through the Lenses of Biomimicry, Industrial Symbiosis, and Green Chemistry"

2.3 Biopolymers for soft materials

Considering that biomedical engineering and healthcare purposes are among the most important application areas for developing soft materials, a smart direction for the efforts in the material's design should be towards non-toxic and bio-based components. Likewise, to reduce the eventual e-waste resulting from the disposal of biomedical devices, biocompatible materials capable of composting after finishing their purpose are only achievable by following green chemistry and a sustainable vision.

In this context, bio-based soft gel materials have been designed with a novel approach to substitute conventional non-recyclable polymers for biobased ones. Biopolymers offer a greener approach owing to their ability to dissolve, resorb, or degrade partially or entirely after their expected working period. [30] Coming from a vast natural stock, naturally derived biodegradable materials like chitosan, cellulose, gelatin, and protein-based polymers are the most utilized ones to soft materials purposes. For instance, chitosan has been used as main component of drug/delivery systems and carboxymethylcellulose is an anionic water-soluble biopolymer capable of forming gels in water. Cellulose biodegradable character along its biocompatibility, softness, transparency, high viscosity and swelling at high pH [31] makes it an ideal candidate as a construction block for soft material's design. Also, gelatin is another biopolymer with diverse advantages, its non-toxicity, high water absorption, biocompatibility and biodegradability allow its use in a variety of healthcare applications. [32]

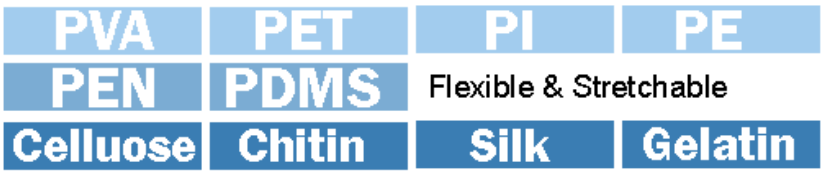

Figure 7. Substrate materials used for flexible electronics. Image by author.

Next, the following sections will describe two biopolymers relevant in the context of designing soft materials, which are of a central topic in this project.

2.3.1 Gelatin

2.3.1.1 Generalities

Collagen is the most abundant protein in humans and animals, where the greatest concentrations can be found in the skin, bones, tendons, and ligaments. Gelatin is a natural biopolymer made through the hydrolytic degradation of protein from collagen and its distinctive structure of amino acids gives it several medical benefits. [33] The major sources of gelatin are pig, cow and fish and, because gelatin derives from raw materials that are byproducts of the meat industry, as long as humankind keeps a meat-based diet, collagen will be a renewable resource available for gelatin production. [34]

In order to properly prepare what we commonly know as *gelatin* from the collagen, a boiling state or a hydrolysis reaction must be performed. Based on the chosen method, two types of gelatins may be produced from the pre-treatment of collagen: Type A or Type B gelatin. The first one is an acid treatment gelatin with an isoelectric point at pH 6 to 9. Type B is obtained through alkaline treatments with an isoelectric point at pH 5, and can be applied to more complex collagen found in bovine hides. [35]

Chemically, gelatin is made up of almost 18 varieties of amino acids, the 57% total is composed of glycine, proline and hydroxyproline, the other 43% belongs to other amino acids families such as glutamic acid, alanine, arginine and aspartic acid. [36] The main constituents of gelatin are polypeptide molecules (chains), where each single chain has a molecular weight of $\sim 90000\ g\ mol^{-1}$ and gets the name of α-chains, the β-chains has two α-chains covalently crosslinked and γ-chains has three forming what is known as the triple helix. [37]

Gelatin is a clear and tasteless protein that has a rheological property of thermoreversible transformation between sol and gel thanks to its triple helix structure. The thermal transition is probably the most useful property of gelatin in solution for different industries and research. [20] When an aqueous solution of gelatin is cooled below 35-40°C an increase in viscosity occurs, then, a gel is formed through three stages: 1) The rearrangement of individual molecular chains into ordered helical arrangement. 2) Association of two or three ordered segments to create crystallites and 3) stabilization of the structure by lateral interchain hydrogen bonding within the helical regions. On the contrary, when gelatin is above 37 ° C, the triple helix conformation returns to the coiled state again and the gel is therefore reversibly melted in a solution.[38]

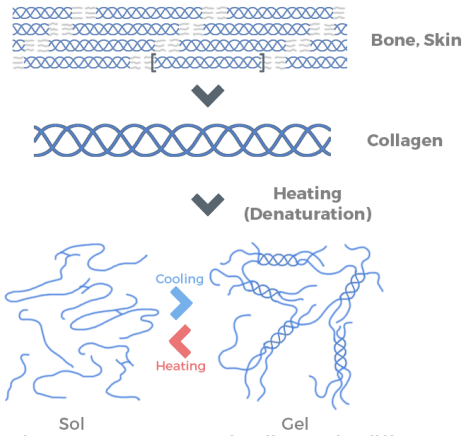

Figure 8. Structure of collagen in different scenarios.

Thanks to its ease molding, biocompatibility, low cost and easy preparation, and its sol-gel transition, gelatin has been widely used in different industries. For example, is general knowledge that gelatin serve as a dessert and a component in food industry because of its gelling capabilities, which also has been used for cosmetics and health products. [39] Collagen and gelatin products have been widely used in the field of skincare. [40] Gelatin is also employed to prepare hydrogels, nanomicrosphere containers, nanofibers and pharmaceutical additives. [41]

Besides a wide palette of applications, gelatin has been proposed in literature as a biodegradable gelator for the preparation of hydrogels, elastomers, e-skin and other different soft material for the design of flexible actuators and flexible electronics. Gelatin based gels are a promising choice because their natural self-assembly behavior avoids the need for additional chemical reactions, allow for water-soluble additives, and are harmless to the environment due to fast degradation and are even edible. [42] Taking advantage of the gelatin's extreme versatility in response to several stimuli, including pH, temperature, mechanically, pneumatically etc., different types of actuators have been proposed. [43] For instance, a gelatin mixture with glycerol and water in a ratio of 1:1:8 resulted in a elastomer that can be cast to create a new type of edible, biodegradable pneumatic actuator. [44] A mechanical actuated gelatin finger was proposed by Harris et al, where the crosslinking gelatin with microbial transglutaminase allows for tuning the stiffness of the material by increasing the Young's modulus. [45] Also, a temperature and humidity responsive flexible scaffold based on gelatin, cellulose and zinc was developed and proposed as bio-degradable e-skin with an *in vivo* response. [42]

Figure 9. Double stimuli response sensor based on a gelatin hydrogel and other biocompatible elements. *Nat. Matter. 19, 1102-1109 (2020).*

2.3.2 Cellulose nanomaterials

Another biopolymer with a huge relevance and tremendous potential for the design of new materials is the cellulose. Cellulose is considered a high-value product with low environmental impact. This natural biopolymer can be found in plants, algae, tunicates and some bacteria. Cellulose is a green, renewable and sustainable material and the most abundant compound on Earth (as an example of its abundance, common wood is composed approximately by 40-50% cellulose). [46] [47] Economically, cellulose represents a cheap natural abundant raw material capable of producing high value products. Indeed, the biomass production reaches 1.5 gigatons (metric ton) annually. [48]

This raw material has a biocompatible and biodegradable non-toxic carbohydrate-based nature. Chemically, cellulose is a high-molecular-weight biopolymer made up of β-1,4-anhydro-D-glucopyranose units where each monomer consists of 3 hydroxyl groups (-OH) to form hydrogen bonds that play a major role in the formation of semicrystalline packing and governs the physical properties of these highly cohesive material. Existing in natural fibers and other plant-based materials, the cellulose's structure has a semicrystalline nature (amorphous and a crystalline regions). [49]

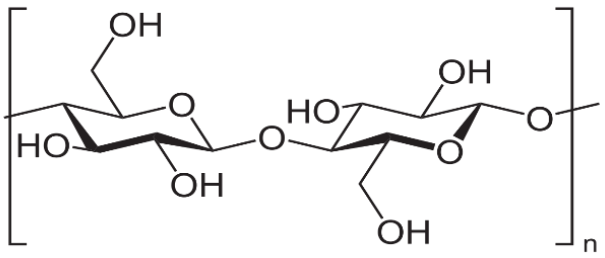

Figure 10. Chemical structure of cellulose.

Cellulose materials have been used since the mid-19th century in various daily life applications, starting from the production of paper, food, biomaterials, pharmaceuticals, and textiles. [50] The application of cellulose is so extensive that its use has been continued nowadays. While cellulose is a vast and rich resource, its economic value can be further increased by the chemical or mechanical extraction of its naturally crystalline regions. These crystalline domains can be isolated apart from the raw material to obtain a high ordered and crystalline block of construction commonly referred as *nanocellulose* or *cellulose nanomaterials.* [46]

Compared to its macro size counterpart, cellulose nanomaterials acquire new physicochemical properties in combination with their naturally renewability and abundance. In addition, they have an excellent stiffness, high strength, low coefficient of thermal expansion, low density, dimensional stability and the hydroxyl groups allows for modification of its surface chemistry. [51] Because of the nanocellulose's tremendous potential, authors like Foster et al. consider the nanocellulose variants as *futuristic materials.* Currently, nanocellulose can be produced industrially at tons per day and can be employed in different fields in our life. Even more, companies like Markets and Markets forecast the nanocellulose market to achieve USD 783 Million by 2025 based on the whole bunch of technological possibilities.[46] For example, nanocomposite materials can be used in biomedical products, adhesives, supercapacitors, template for electronic components, batteries and catalytic supports, another applications include electroactive polymers, fibers and textiles, food coatings, antimicrobial films, cosmetics, and plenty more applications. [52][53]

2.3.2.1 Cellulose nanocrystals

It is important to mention that different number of nanocellulose variants can be isolated depending on the method and the natural source, the most common are nanofibrillated cellulose (NFC), rigid bacterial nanocellulose (BNC) and cellulose nanocrystals (CNCs). CNCs, for example, derive from a controlled strong acid hydrolysis treatment using mineral sulfuric (H_sSO_4), hydrochloric (HCl) and phosphoric (H_3PO_4) acids. This technique has been employed as the most common method to dissolve the amorphous regions of cellulose to yield CNC. [54] Briefly, during the acid hydrolysis the hydronium ions penetrate the cellulose chains through the amorphous regions, promoting then a hydrolytic cleavage of the glycosidic bonds and releasing individual crystallites. [47]

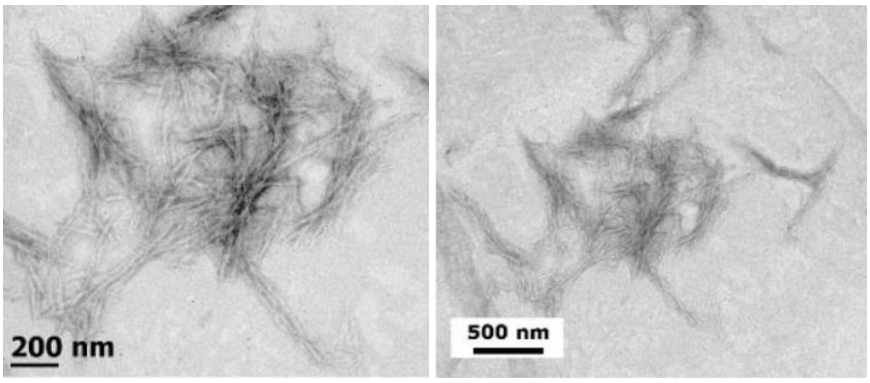

Figure 11. TEM Micrographs of CNCs from CelluForce™. ACS Sustainable Chem. Eng. 2021, 9, 45,

Cellulose nanocrystals (also known as *nanowhiskers*) are nanostructures defined as stiff, rod-like nanosized materials with a lightweight character. [55] because of its outstanding features this nanomaterial has attracted a lot of attention recently: their nanoscale dimension grafts them a large surface area (250-500 m^2/g), a high tensile strength (~7500 MPa) and a Young's modulus of ~100-140 GPa. [48] CNCs also have noticeable optical properties. CNCs are isotropic and beyond a critical concentration in aqueous solutions the alignment of the crystals can change the polarization of the transmitted light due to a phase difference. This birefringence effect is attributed to the alignment of cellulose chains within the CNC, therefore, this morphology is responsible for creating an optical axis in the CNC, which results in the polarization of transmitted light. [56]

CNCs also display a high thermal stability ($\sim 260\,°C$) a high aspect ratio of $\sim 10-70$ length-diamter (*L/D)* and, as a direct consequence for the hydrolysis with strong acids, the CNC's surface is grafted with anionic sulfate half esters groups ($-OSO_3^-$), imparting them with a highly negative zeta (ζ) potential and, therefore, a great colloidal stability in aqueous systems. [57] Nonetheless, CNCs still retain its biodegradable and biocompatible character, making it a suitable for soft materials applications where sustainability is a matter of concern.

Because of all the remarkable properties CNCs have, they are commonly used as fillers or reinforcement agents in different nanocomposite and the application in soft materials is not the exception. In fact, soft tissues in biological systems are hierarchical fiber-reinforced soft materials. For example, articular cartilages, a biological hydrogel with water content up to $\sim 90\%$ have strength up to 30 MPa with an extension at break of $\sim 100\%$ owing to their composite structure that collagen fibrils reinforce a proteoglycan matrix. [58] As soft materials follow a bio-based approach, it's not a surprise that CNC and carboxylated CNC are used as nanofillers to increase the mechanical, thermal, or optical properties in different types of soft materials.

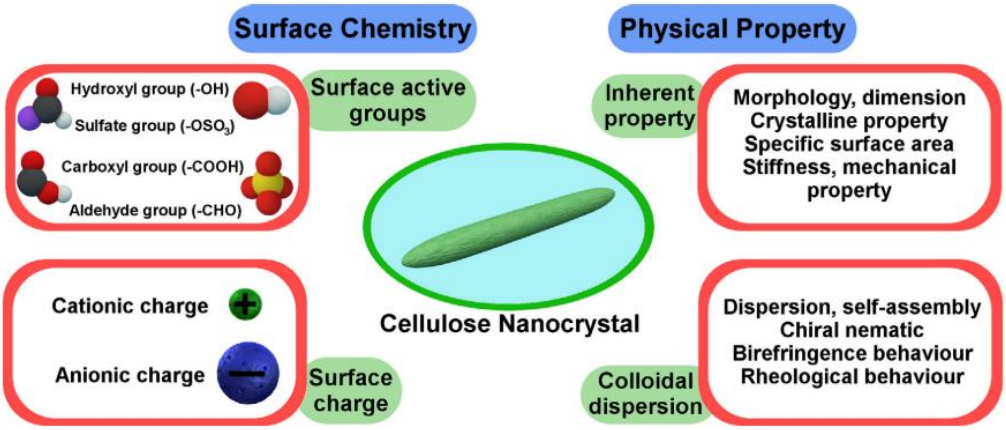

Figure 12. Physical and chemical properties of CNCs. *J. Colloid Interface Sci.,* vol. 494

2.3.2.2 Surface modification of cellulose nanocrystals

Because of the CNCs are at nanometric dimensions (an average of 3-50 nm width and 50-500 nm in length), the surface chemistry plays a crucial role in the material. As mentioned before, the obtention of CNCs is achieved through an acid hydrolysis treatment which grafts the surface with an anionic charge of OSO_3 groups (termed as S-CNC). Even if the CNCs get a negative charge and therefore a good stability in water, a high concentration of these groups has been observed to influence negatively in the thermal stability of CNCs and, also, they may be an impediment to include other desired functional groups on the surface. [50] In consequence, the surface modification of a wide variety of cellulose nanomaterials has become a very investigated research topic. Some examples include the acetylation and the silylation of the cellulose in order to increase the hydrophobicity of the material. For example, Çetin et al. functionalized the CNC surface with acetyl groups through a transesterification of vinyl acetate, and Zhang et al. developed highly flexible silylated-nanofibrillated cellulose sponges with hydrophobic and oleophilic properties, perfect for dodecane spills remotion. [59] [60]

Recently, the incorporation of carboxyl groups on the cellulose surface. The carboxylated cellulose nanocrystals (cCNC) share a similar colloidal stability, uniform scale lengths and crystallinity compared to the sulfate half-ester CNC. The carboxyl cellulose, similar to the S-CNC, possess anionic groups that promote the electrostatic repulsion between neighboring CNCs, therefore preventing the aggregation of the nanoparticles. [61] Also, the replacement of the OSO_3 groups for more hydrophilic functional groups, open the door through a possible non-covalent

interaction among the CNC and a matrix (commonly a solvent) or a second component in a material, where the rich surface chemistry and high surface area enable the CNC to be a structural support for the production of new nanocomposites granting them with improved properties. To mention some examples, Chen et al. developed a polypyrrole (PPy)-cCNC flexible film for personal electronics and, as expected, the addiction of the functionalized CNC increased the mechanical strength of the films. Cao et al. developed cassia gums for edible packing using cCNC and, while there was no evidence of covalent interactions, the inclusion of up to 4% cCNCs to the films improved the mechanical properties, the heat seal strength and the oil permeability. [33] [34]

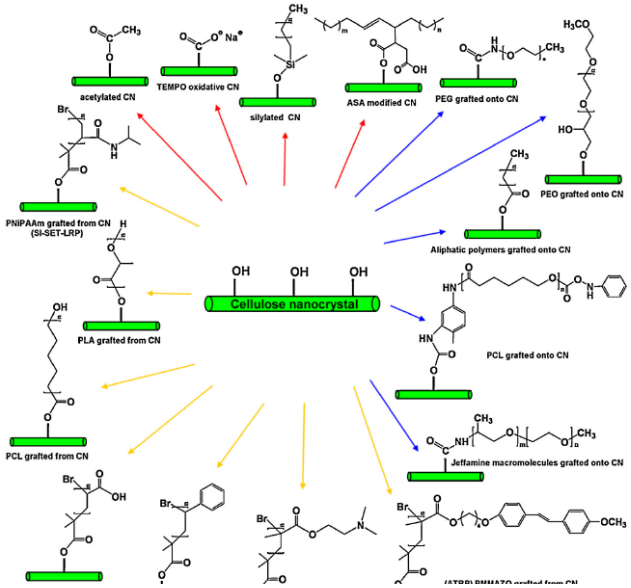

Figure 13. Common surface chemical modification of cellulose nanocrystals. Mater. Today, vol. 16, no. 6, pp. 220–227, 2013

In the literature, the 2,2,6,6-tetramethyl-1-piperidinyloxy (TEMPO)-mediated oxidation reaction is the most common method to modify the cellulose's surface to incorporate anionic carboxylate groups on the surface of the nanocrystals. The TEMPO mediated reaction involves the application of a stable nitroxyl radical (TEMPO) in the presence of NaBr and NaOCl. Its applicability on CNCs was first reported by Vignon et al., the methodology consist on the S-CNC being subjected to a mixture of sodium hypochlorite, sodium bromide, and TEMPO for the selective oxidation of the primary surface hydroxyl groups to produce carboxylated CNS [64] Other common methods include the oxidation through hydrogen peroxide in a one step process and the functionalization using a transition metal-catalyzed oxidation process. Despite followed methodology, different techniques

have been used to calculate the carboxylic content on the cellulose's surface, including conductimetric titrations, FT-IR and methylene blue adsorption methods are the most used, where the carboxylic content is calculated in $mmol\ kg^{-1}$ or $mmol\ g^{-1}$. The previously described methods and some others are described in Table 1.

Table 1. Methods for carboxylation of cellulosic nanomaterials.

Method	Reagents	Average Carboxylic content $(mmol\ g^{-1})$	Reference
TEMPO	NaBr NaOCl	0.2 – 1.0	[61]
APS	Ammonium Persulfate	0.6 - 1.4	[65]
Hydrogen Peroxide	H_2O_2 (30%)	0.12 – 0.2	[61]
Metal-catalyzed oxidation process	$NaOCl/NaOCl_2$	0.15	[61]
Deep eutectic solvents	Oxalic Acid/Choline Chloride	0.2 – 2.44	[66] [54]

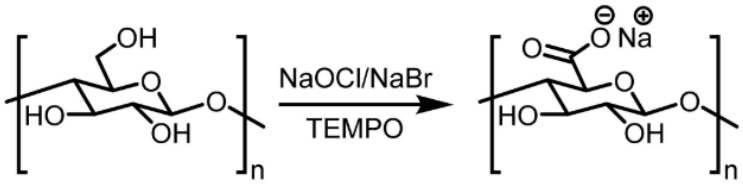

Figure 14. TEMPO oxidation of CNCs.

While the TEMPO-mediated reaction is the most used and efficient method for producing carboxylic cellulose nanomaterials, the fact is that the cellulose oxidation produces a large amount of salt-containing wastewater [66]. Therefore, an alternative option must be considered to develop a sustainable, environment, friendly cellulose carboxylation method. As mentioned in the previous table, the DESs are presented as a greener alternative to traditional methodologies. Briefly, DESs are low cost, highly efficient, green, environmentally friendly ionic fluids composed of a mixture of hydrogen bond donors (HBDs) and hydrogen bond acceptors (HBA) with reduced melting point related to the pure components. It has been reported that cellulose nanomaterials can not only be functionalized is DESs but also to be prepared in situ, something that is not possible through TEMPO reaction. However, more about this methodology will be described in the following sections.

2.4 Deep Eutectic Solvents

2.4.1 Generalities

Since the concept of “deep eutectic solvent” (DES) was introduced in early 2003 by the Abbott group, [67] the development of these new tunable green solvents has been crucial for the growth of non-aqueous chemistry and a pivot for green chemistry as well. Though the definition of deep eutectic solvent could be aboard through different perspectives, the Abbott group defines a DES as *“a system formed from a eutectic mixture of Lewis or Bronsted acids and bases which can contain a variety of anionic and/or cationic species”*. [68]

DES are often considered as binary or ternary mixtures of compounds capable of associating mainly via hydrogen bonds. Formed by at least two components, a hydrogen bond acceptor (HBA) and a hydrogen bond donor (HBD), the HBD and the HBA are capable of self-associate to form a brand-new liquid phase. [69] Through the complexation of a quaternary ammonium salt (HBA) with a metal salt (HBD) the newly formed solvent is known for containing large, nonsymmetric ions with low lattice energy, so called type I DESs. Thus, a charge delocalization occurring through hydrogen bonding of the components is responsible for the decrease in the melting point (or freezing point) of the mixture with the characteristic of being abnormally lower than that of each individual component. [68]

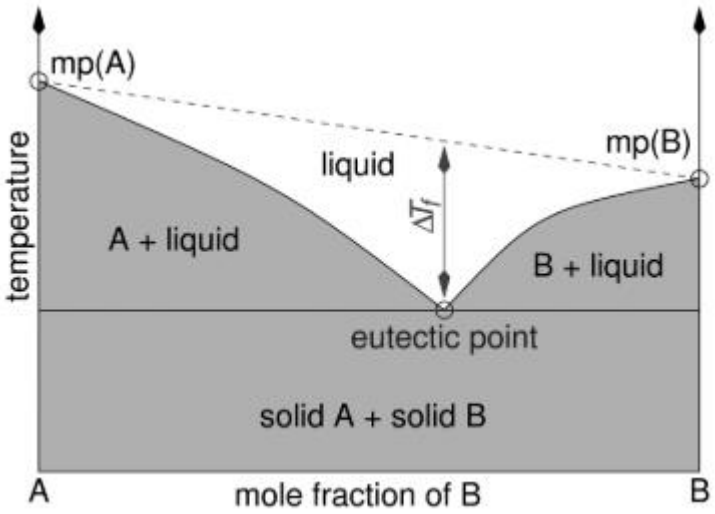

Figure 15. A common binary phase diagram for eutectic mixtures.
Chem. Rev. 2014, 114, 21, 11060-11082.

As DES can be prepared with diverse types of compounds, they are categorized into four distinct types based on the general formula:

$$Ca^{+}X^{-}zY$$

Where Ca^{+} is an ammonium/phosphonium/sulphonium, X^{-} is a Lewis base, Y is a Lewis or Bronsted acid and z is the number of Y molecules. Type III DES are the most common and most studied systems in literature, they consist of a quaternary ammonium salt and a HBD, typically an organic molecule (amides, carboxylic acids or polyols). [70] Considering its low cost, biodegradability and low toxicity, the most common organic salt (HBA) used to produce Type III DES is the choline chloride (ChCl), whereas urea, glycerol and ethylene glycol serve as common HBDs. [26]

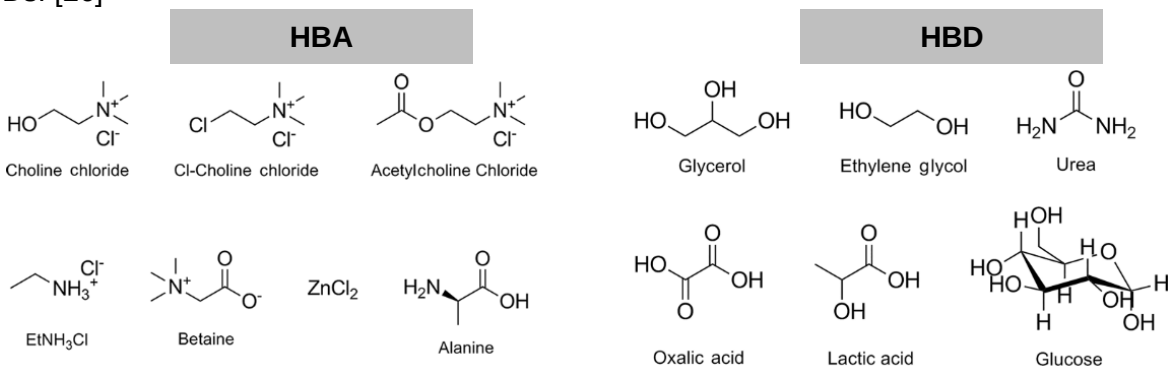

Figure 16. Example of hydrogen bond acceptors and donors usually employed in the synthesis of DES. *J. Inorg. Chem., 2015. 5147-5157*

DES are typically described as viscous, clear liquids with certain tonalities depending on its main constituents which, in fact, comprise a broad set of safe, renewable, inexpensive and biodegradable components capable of forming an enormous variety of eutectic solvents.[71] As described by Mecerreyes "*Only in the last 5 years DES have become popular due to the sustainable and economically viable approach to alternatives to expensive ionic liquids*." [16]

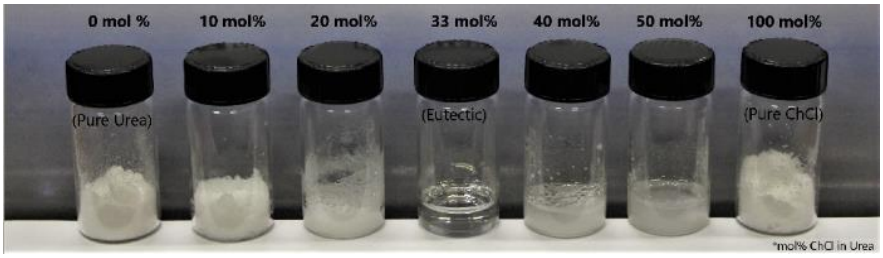

Figure 17. Urea:ChCl DES can only be obtained at certain molar composition. *Chem. Rev. 2021, 121, 3, 1232-1285.*

Many of their characteristics are consequence of its extensive hydrogen bond network, such as their low melting points (T_m), dipolar nature, high solubility of resilient solutes and tunability; [72] their low vapor pressure, chemical and thermal stability, relatively wide liquid-range, nonflammability and ease storage represent no security issues during its synthesis. [68] Also, DES show extremely low toxicity and no purification steps are required after its preparation by simple mixing. Finally, in efficiency of preparation terms, DES are capable of achieving 100% conversion (atom economy), [16] recognized as one of the 12 principles of green chemistry.

DES are considered as *design solvents* whose characteristics can be tailored and customized as desired by varying the composition of the mixture. Some physicochemical properties like T_m, viscosity, pH and conductivity are highly related to the type of salt and HBD used as well as the mole ratio of both compounds. [68] As can be seen from Table 2, properties strongly depend upon the HBD in the DES. For instance, the ethylene glycol:choline chloride DES (also known as ethaline) has the highest conductivity among the most studied DESs, whereas the oxalic acid and urea DES (reline) are known for having high viscosities.

Table 2. Physicochemical properties of Type III DES.

HBA	T_f *°C*	*HBD*	T_f *°C*	*Molar ratio (HBA:HBD)*	*DES* T_f *°C*	*Conductivity* $(mS\ cm^{-1})$	*Density* $(g\ cm^{-3})$	*Viscosity* (cP)	*Ref*
ChCl	303	Urea	134	1:2	12	0.75	1.24	632	[67]
		Glycerol	290	1:2	16.85	1.05	1.18	36	[73]
		EG	-12.9	1:2	-36.15	7.61	1.12	49	[73]
		Oxalic Acid	190	1:1	34	0.38	1.15	597	[73]

2.4.2 DESs Applications

DESs are versatile mixtures that can be applied in multiple science and engineering areas. Originally, DES were designed for metals and metal salts extraction due to its high solubilities and electrical conductivities in the solvents, making them good candidates for extraction of metals in solution [74], ore refining [75] and electrodeposition [76]. Other applications include liquid-liquid extraction of azeotropic mixtures where a ChCl:levulinic acid DES was used to separate ethanol from heptane. [77] DES have also been used as electrolytes for the design of lithium-ion batteries (LIBs) owing to their suppressed flammability, wide liquidus range, and high conductivity. [78] In the area of medical research and pharmaceuticals, the ability of the DES to dissolve certain

compounds that are particularly difficult to dissolve in water has been explored. For example, Morrison et al. discovered that reline and malonic acid DES achieve a solubility 22000 times greater than water for several solutes, including benzoic acid, danazol, itraconazole etc. Another example is the research performed by Lu et al., where they demonstrated that the solubility of aspirin, acetaminophen, ketoprofen, naproxen, and ibuprofen is higher and only achievable in DES than its pure components by themselves. [79] More recently, DESs have been incorporated into the development and research for producing different kinds of nanomaterials. Due to its extended network of H-bonds and its wide range of temperatures, DES have been used as reaction media for the synthesis of self-assembled Au nanostars [80], nanostructured Ni films [81], and as dispersant of nanoparticles and other nanocomposites.

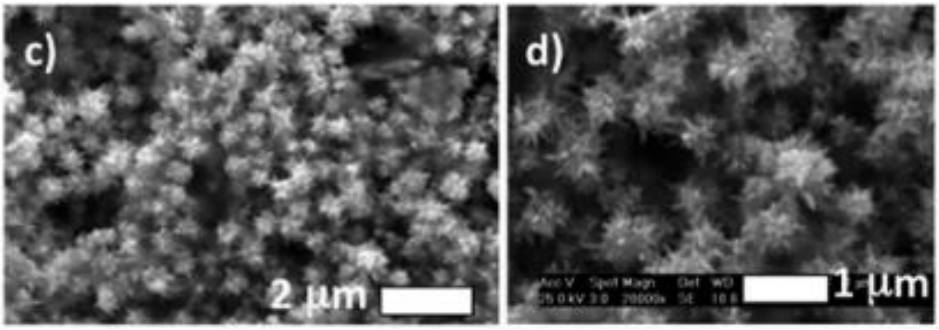

Figure 18. Gold nanostars obtained in a reline DES. Recovered from: J. Matter. Chem. A, 2015, 3, 15869

Deep eutectic solvents have a tremendous potential and are relevant in many areas of science and, while only a few examples were mentioned, the next sub sections will focus in two specific applications which concern to this project.

2.4.2.1 DES for cellulose functionalization

DESs have been used for the dissolution and dispersion of cellulose nanomaterials. Previous studies of cellulose dissolution using ionic liquids attribute this characteristic to the solvent's properties derived from H-bonding, other research focused on DES promoting the cellulose dissolution using oxalic acid-ChCl, citric acid/ChCl, urea/ChCl and concluded that H-bonding along with a large number of remaining ions could form hydrogen bonds with the OH groups of the cellulose, resulting in the efficient dissolution of the biopolymer. [82][83] Compared to the traditional TEMPO reaction method, because of the DES biodegradable nature, this method has the advantage of low cost, high efficiency, low toxicity and easy degradation.

Hence, DESs have been proposed as a green alternative for the synthesis and dissolution media for cellulose nanomaterials, including the functionalization or incorporation of anionic carboxylic groups on the celluloses' surface. However, only a few methodologies have been described in literature, for instance, Sirviö et al. proposed acidic DESs for cellulose nanocrystals production where the carboxylic content was calculated by a conductimetric titration recaching a carboxylic content about $\sim 0.2 - 0.27\ mmol\ g^{-1}$. [54] On the other hand, a recent methodology proposed by Cao et al. studied different factors for the synthesis and carboxylation of cellulose nanoparticles like the DES molar ratio, the size of the particles and the reaction time. [66] Besides differences may exists between the methodologies, both can be summarized as follows: different concentrations of cellulose nanomaterials are suspended in an acidc DES (typically, anhydrous oxalic acid or oxalic acid dihydrate) and stirred for a certain time. After the reaction time is over, the cellulose is washed 4 or 6 times to remove the DES, then the cellulose is suspended in water and freeze dried for a day. While the cellulose is stirred in the DES, it is proposed that the carboxylic acids from the oxalic acid undergo an esterification reaction between carboxyl groups and hydroxyl groups on the cellulose surface of cellulose to form carboxyl groups thereby improving the physicochemical properties of cellulose. [84]

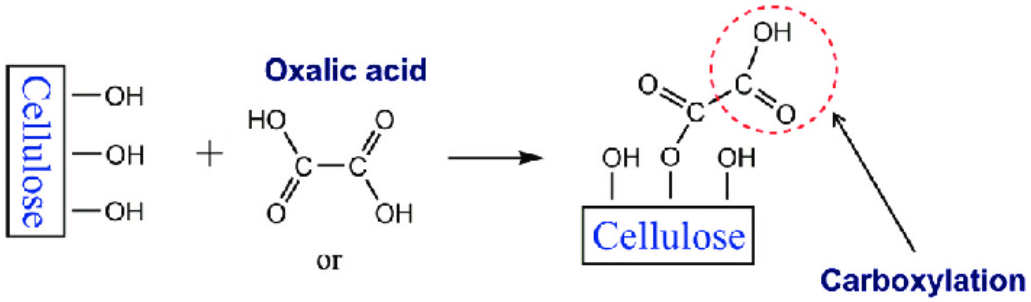

Figure 19. Surface modification of cellulose in a deep eutectic system.

2.4.2.2 DES for eutectogels design

Briefly mentioned in section 2.2, DESs were recognized as crucial solvents to develop the next generation of flexible electronics and soft devices. Even though ILs have been well explored as electrolyte for soft materials, their toxicity and high manufacturing cost is a challenge that can be overcome by moving towards a greener, cheaper, and renewable options like DESs are.

Firstly reported by Joos et al., eutectogels consist on the immobilization of a DESs in a solid matrix. Previously, eutectogels were labeled as a new class of solid composite electrolyte (SCE), useful in flexible batteries and capacitors. [85] Through the years, the concept of *eutectogel* has

shifted to a different class of gel (or soft matter) which, upon the addition of a second component (a gelator), a transition to gel occurs. [10]. The vast number of non-covalent interactions in the DES is essential to the formation of the gel matrix where H-bonding is the most commonly employed non-covalent driving force as assembly strategy for eutectogels reported to date. [18]

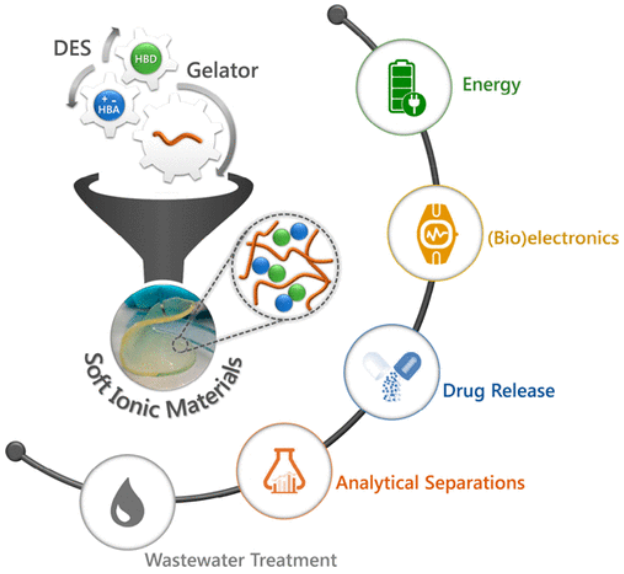

Figure 20. Three-dimensional network where the DES is the predominant solvent. J. Phys. B 2020, 124, 8465-8478

Interestingly, these gel materials usually preserve the intrinsic properties of the dispersed liquid phase, including thermal stability, low volatility, non-flammability, high ionic conductivity, among others. The properties of eutectogels can be tailored by changing the chemical structure of the DES and the gelator, the ratios between them, as well as the nature of interactions (covalent or no covalent) and the cross-linking degree. [16] Authors like Mecerreyes recall the importance of the relation that exists between the DES and the gelator, for example, the elastic modulus increase significantly when increasing the polymer scaffold, due to an increase of polymer entanglement density. Also, the conductivity of an eutectogel is higher when the DES is close to the maximum concentration. It is also worth mentioning that, because of the high number of H-bonds and non-covalent interactions in the DES, new characteristics like shape-memory and self-healing properties may appear in the materials.

Through this gel-assembly strategy, different types of gelators have been used: linear polymers, polymer networks, biopolymers, supramolecular compounds, or sol-gel derived silica networks. Some examples include the work proposed by Mortharpour et al, who developed stable

ionic soft materials using HEMA in a ChCl:Ascorbic acid (2:1) to contain anticancer drugs. [86] Other works involve the addition of a ethaline DES into a chemically cross-linked polymer scaffolds formed via UV curing of HEMA and PEGDA for supercapacitors applications. [86] Zheng et al. were deeper in the development of wearable devices and proposed the design of deep eutectic polymer (DEP) blends with polyvinyl alcohol (PVA), reaching a very transparent, fully recyclable highly stretchable material with applications as a strain, temperature and humidity sensor. [87]

Figure 21. DES/PVA polymer blend. ACS Applied Materials & Interfaces 2022 14 (43), 49212-49223.

Taking advantage on their natural origin as well as their renewable, cheap, biocompatible and nontoxic nature, biopolymers have been reported as excellent gelators for the design of green soft materials. Biopolymers are highly abundant in nature, and because of their inherent self-assembly strategies, they can be easily exploited for the formation of 3D networks within specific DESs. The presence of ions as well as the H-boding in the DES makes it possible to dissolve and disperse resilient and complex polysaccharides like cellulose, chitin, gelatin, liginin and starch, among many others. [10]

To mention some examples Zeng and collaborators prepared xantham gum eutectogels in a ChCl-Glycerol/Xylitol/Sorbitol/Citric acid DES, increasing the thermal stability of the gel up to 80 °C. [88] Panzer et al. presented a gelatin-based eutectogel in a ethaline DES exploiting the thermally modulated coil-helix transition process of gelatin by heating and cooling the mixture. The obtained eutectogel resulted highly stretchable, transparent, nonvolatile and highly conductive because of the inherent solvent's conductivity ($7.6\ mS\ cm^{-1}$) and also a strain-sensor wearable device was proposed as a proof of concept. [89] Additionally, this work in fact demonstrate that a DES outperform the aqueous environment for the formation of new materials, whereas the eutectogels

could containing 22 wt% of the gelator exhibiting a 300% fracture strain while their analogous hydrogels only reached 90%.

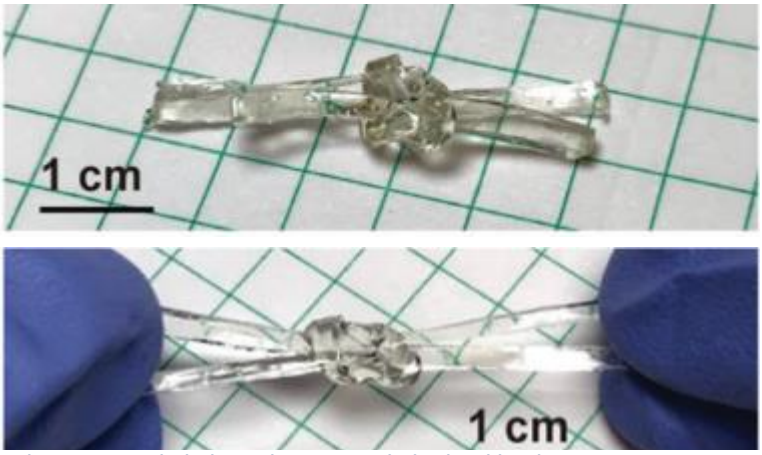

Figure 22. Gelatin based eutectogel obtained by the Panzer group. J. Mater. Chem. C, 2019, 7,601

In short, deep eutectic solvents have demonstrated similar properties to ILs (ionic conductivity, self-healing, stretchability), where the advantage over this type of liquids is found in their biobased nature, nontoxic character, simple preparation and versatility in their preparation. Eutectogels have been proposed as soft materials for applications in flexible electronics and wearable devices whose elastic and conductive character can be tailored by controlling the crosslinking density as well as choosing the right polymer and the ideal DES according to the desired necessities. Even if eutectogels already display outstanding and a wide gamut of marvelous attributes, those characteristics can be improved by the judicious addition of a third component. If additional modification of the mechanical, rheological or optical properties is desired in the gels, the addition of nanomaterials into the gel matrix is a promising strategy to explore. Based on the previous statement, in section 2.3.2 it was mentioned that the high surface area, abundance of hydroxyl groups and other mechanical properties make cellulose nanocrystals a suitable and versatile filler for different polymeric matrix, therefore it can be used as a bio-based building block for the construction or reinforcement of biodegradable flexible devices in deep eutectic solvents.

However, besides all promising developments made in the eutectogels design in recent years, the fact is that hydrogels still stand out as the top of the scientific literature among all gel materials. Nonetheless this gap in knowledge it’s a big opportunity to further extend the research about eutectogels, biopolymers, and their combination with nanomaterials for the development of new green and sustainable soft materials for the next generation of flexible devices.

3. Hypothesis

The addition of cellulose nanocrystals with different surface chemistry to a gelatin-based eutectogel will increase the number of non-covalent interactions, therefore improving the mechanical properties of the system.

4. Objective

4.1 General objective

To design, characterize and evaluate a gelatin-based ionic soft material reinforced with cellulose nanocrystals with different functionalized surfaces.

4.2 Specific objectives

- To modify the CNC's surface chemistry through a functionalization technique in an oxalic acid-based deep eutectic solvent.
- To optimize the preparation of the previously reported 22 wt% gelatin eutectogels.
- To prepare cellulose-eutectogel composites having different cellulose concentrations using both commercial (sulfate-functionalized) and carboxylate-functionalized cellulose.
- To characterize the obtained eutectogels through different characterization techniques: FTIR, EIS, UV-Vis spectroscopy, DSC and mechanical characterizations.

5. Methodology

5.1 Materials

For the ethaline and oxalic acid DES preparation, ethlylene glycol (anhydrous, 99.8%), oxalic acid dihydrated (ACS reagent, $\geq 99\%$) and choline chloride (ACS reagent, $\geq 99\%$) were purchased from Sigma-Aldrich. To remove possible traces of water from the choline chloride, it was oven-heated in a Pyrex glass bottle to 90°C for 24 h, afterwards, the bottle was sealed until its posterior use. Type A gelatin from porcine skin (~175 g Bloom) from Sigma-Aldrich and cellulose nanocrystals (CelluForce NCC®) were used without any further purification.

5.2 Experimental design

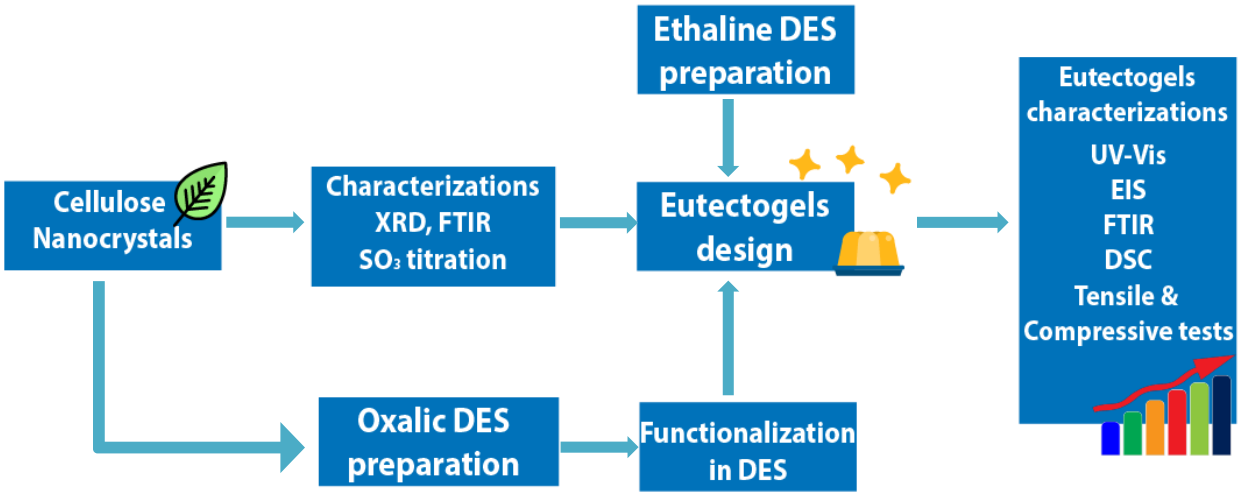

Figure 23. Step-by-step followed methodology.

5.2.1 Deep eutectic solvents

5.2.1.1 Ethaline DES preparation

The preparation of deep eutectic solvents has been previously reported in the literature. The methodology was followed as described by Vatanpour et al. [90] Briefly, the Ethaline DES was prepared by mixing the ethylene glycol and choline chloride in a molar proportion of 2:1, respectively, in a glass container. The mixture was heated under heating up to 75°C until a transparent, homogeneous, and colorless liquid was obtained. The container was then sealed until its use.

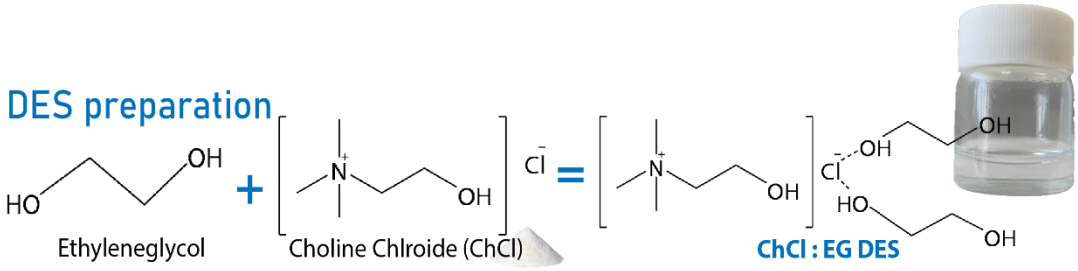

Figure 24. Methodology followed for the Ethaline preparation. Image by author.

5.2.1.2 Oxalic acid DES preparation

A choline chloride-oxalic acid dihydrate DES was prepared like the ethylene glycol DES with minor differences. Both components were mixed in a 1:1 molar ratio and stirred under vigorous stirring while heating up to 60 °C until a mixture like ethaline was obtained (homogeneous, transparent and colorless).

5.2.2 Cellulose nanocrystals

5.2.2.1 COOH functionalization

It is important to note that the carboxylation of CNCs (cellulose nanocrystals) using deep eutectic solvents has been rarely been reported in literature; thus, a method described by Juho et al. was followed. [54] First, in the previously prepared oxalic acid DES, 5 wt% of CNC with respect to the DES, was added and the mixture heated up to 60°C for 3 hours under vigorous stirring. At determinate times of reaction, the reaction was stopped. The reaction mixture was then washed 6 times with ethanol (10 ml) and the conductivity of the washes was measured with a *HANNA Instruments EDGE potentiometer* between each wash to make sure the DES was completely removed. Finally, the CNC was resuspended in ethanol for its further use to avoid drying and undesired agglomerations.

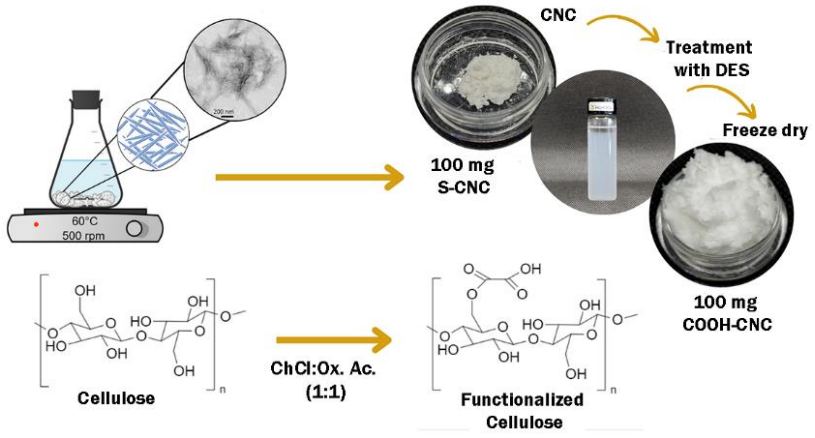

Figure 25. Edited from: “Desarrollo de geles basados en celulosa monocristalina modificada en sistemas eutécticos profundos para el cultivo 3D de calculas.” Poster presented during the “XXXV Congreso Nacional de la SPM. Monterrey.” October 17, 2022. A. G. Blanco.

5.2.2.2 Calculation of sulfate and carboxylic groups

To calculate the concentration of sulfate (S-CNC) and carboxylic groups (COOH-CNC) in the cellulose, a conductimetric titration was performed using a 1 wt% CNC solution in water (pH 7) at room temperature. For these systems, it is critical to recognize the type of charged groups, for weak acids (-COOH) or strong acids ($-OSO_3H$) distinct titration procedures must be followed. As different protocols have been designed and presented in literature, the following procedure is described in ***Chem. Soc. Rev., 2018, 47,2609.*** [91] As ionic conductivity is directly proportional to the amount of electrolytic solution it is essential that the measured conductivity be corrected for the volume of NaOH added at each data point using the following equation:

$$Conductivy_c = Conductivity_m \, x \, \left(\frac{V_i + V_0}{V_i}\right)$$

5.2.2.3 Protocol for strong acids titration

10 mL of 1 wt% S-CNC suspension is diluted in 198 mL of DI water; the mixture is stirred until aggregates are no longer visible. Shortly after, 2 mL of 100 mM NaCl solution is added to set the conductivity to a measurable range (pH of 6). In 100 μL intervals, 10 mM NaOH is titrated while the conductivity is measured repeatedly, making sure that 30 to 60s pass during each titrant's addition. The conductivity was measured with a potentiometer placed in the CNC suspension. Once the equivalence point is reached, the excess NaOH recorded data allows for a statistically significant linear regression where the equivalent molar charge is calculated via the molar volume of NaOH added, defined as the intersection point of the linear regression of the regions before and after the equivalence point. The experiments were performed at least in triplicate.

5.2.2.4 Protocol for weak acids titration

To 10 mL of 1 wt% COOH-CNC, 1 mL of 100 mM HCl was added and diluted to 200 mL with DI water (pH of 3). 1 mL of 100 mL was added for every 0.1 g of CNC contained in the suspension. The solution was then titrated with 100 μL additions of 10 mM NaOH while continuously measuring the pH and conductivity. In this type of titration, the titration curves exhibit two equivalence points as a change in the slope. The molar surface charge is calculated as the molar volume of NaOH added between the strong acid and weak acid equivalence points. As the equivalence points are not sharply defined as in the case of the previously described S-CNCs, the equivalence points are determined as the intersection points of linear regressions of the strong acid plateau and excess

NaOH regions. The molar volume of NaOH added between these intersection points is equivalent to the molar surface charge of the CNC.

5.2.2.5 X-ray diffraction (XRD)

To confirm the crystalline character of the cellulose, an XRD analysis was performed to a cellulose powder sample using a Rigaku Ultima IV XRD equipment at 30mA and 40 kV (CuKα $\lambda = 1.5406$ Å). The diffraction data was collected from $2\theta = 4\ to\ 60°$ at a scanning rate of $4\,° \, min^{-1}$ and compared with the JCPDS card No. 50-2241.

5.2.3 Eutectogels preparation

Previously reported in the literature, the Panzer group proposed a methodology for gelatin based eutectogels using ethaline and glycine as solvents and electrolytes. [89] [92] Briefly, a 22 wt% gelatin solution was prepared in ethaline DES under slow stirring to avoid the bubble formation and heated up to 75 °C for 1 hour until a yellowish yet transparent mixture was formed. For the CNC reinforced eutectogels, prior to the DES addition, 1 wt% (of the total solution) S-CNC or COOH-CNC was added to the mixture, where the solutions acquired an opaque character due to the cellulose presence in the eutectogel. Hereafter, all solutions were then casted in different molds depending on their future use. The eutectogels solution precursors were let to gel to 4 °C for a day.

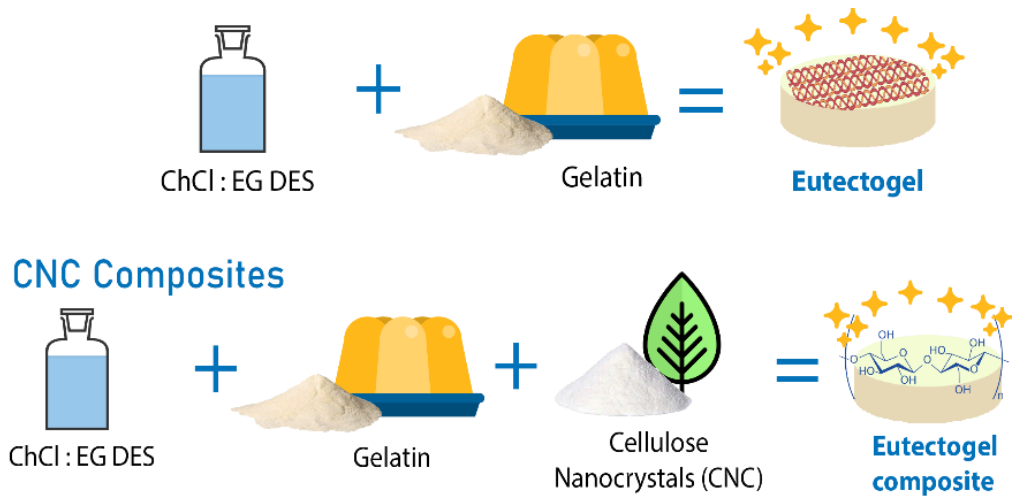

Figure 26. Eutectogels and reinforced CNC eutectogels preparation. Image by author.

5.2.4 Characterizations

5.2.4.1 UV-Vis spectroscopy

The transmittance spectra of different eutectogels samples of 2 mm thickness were recorded using an UV-vis spectrophotometer Thermo Scientific 8420-208200 in a range of 400-800 nm. The cylindrical samples were attached to a side of the quartz cuvettes, the neat ethaline DES was used as a blank for the measurements.

5.2.4.2 Mechanical Characterizations

A universal testing machine Zwick/Roell Z005 was used to measure the samples stretching (%) and compression. The eutectogels were cast on a PTFE ASTM probe mold (2.52 x 4 x 23.64 mm) kindly donated by Prof. Panzer from Tufts University. Tensile tests were conducted at 4°C at 50 mm /min and compressive tests of 4.5 mm thickness samples were conducted at 20 mm/min at room temperature.

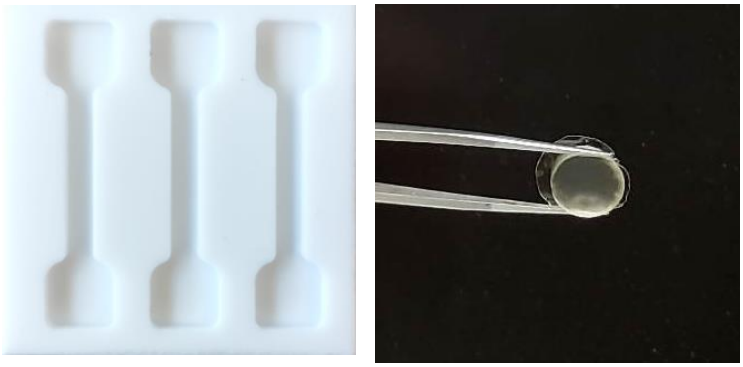

Figure 27. PTFE mold used for the tensile tests (left). Cylindric 4.5 mm thickness samples used for the compressive tests (right).

5.2.4.3 Electrochemical impedance spectroscopy (EIS)

In collaboration with Tufts University, the eutectogel's electrical characterizations were performed under the tutoring of Dr. Matthew J. Panzer from the Chemical and Biological Engineering Department. AC Impedance spectroscopy was performed to measure the contribution of the DES ionic conductivity in the eutectogels, using a VersaSTAT potentiostat with a built-in frequency response analyzer (Princeton Applied Research). Gel precursor solutions were poured into a custom-built Teflon cell array with gold-coated electrode pins and cooled via refrigeration overnight at 4°C in the array. Room temperature AC impedance spectroscopy measurements were performed over the frequency range of 1 Hz to 300 kHz using a sinusoidal voltage amplitude of 10

mv (with a 0 V DC offset). The cell constant used to convert impedance at high frequency to ionic conductivity was determined by calibration using three different neat ionic liquid electrolytes with known conductivity values. At least three replicates eutectogels with different CNC concentration were tested, and the average values were calculated to determine ionic conductivities. The used equation is as follows:

$$\sigma = \frac{1}{\rho} \cdot 3670$$

where σ is the ionic conductivity, ρ is the material's resistivity and 3670 is the cell constant used to correct the conductivity.

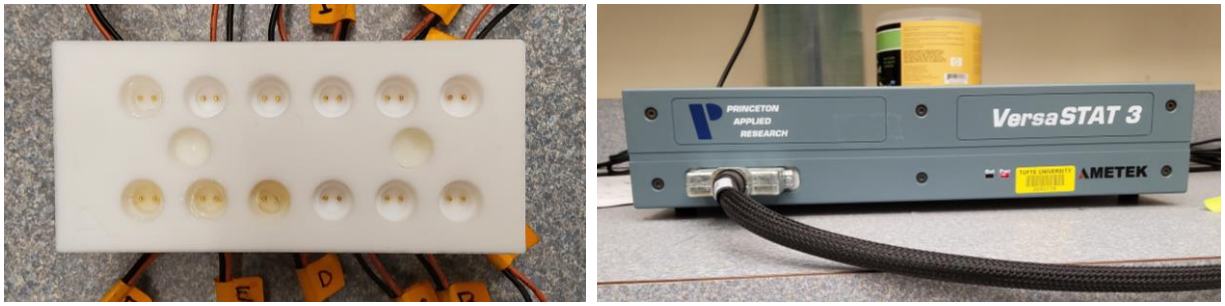

Figure 28. Custom-built PTFE array designed by the Panzer Group. Tufts University Department of Chemical and Biological Engineering. Princeton Applied Research VersaSTAT 3 used for the EIS tests.

5.2.4.4 Differential scanning calorimetry (DSC)

Differential scanning calorimetry measurements were carried out using a Mettler Toledo calorimeter model DSC3+ previously calibrated with Indium. Scans were carried out at 10 °C min^{-1} under nitrogen flow. First, the samples were cooling from room temperature to -20 °C, then, the temperature was maintained at -20 °C for 10 min, after, the temperature was raised to 230 °C, and finally decreased from 230 °C to room temperature at the same temperature ratio.

6. Results and discussion

6.1 Cellulose

6.1.1.1

As the cellulose's crystallinity index may vary depending on the batch prepared, X-ray diffraction technique was used to investigate the crystallinity structure of the CNCs (CelluForce NCC®). The powder sample from CelluForce™ exhibited typical diffraction peaks at approximately 2θ values around 15.3, 16.5 and 22.5° (Figure 29), attributed to the planes (1-10), (110) and (200), respectively, therefore confirming the characteristic diffraction peaks of the cellulose. [93]

To calculate the relative crystallinity index (CI), the Segal's equation was used. I_{max} represents the intensity of the crystalline plane (200) and I_{am} represents the intensity of the baseline at $2\theta = 18°$:

$$CI = \frac{I_{200} - I_{am}}{I_{200}} x\ 100 = \frac{12000 - 2000}{12000} x\ 100 = \ 83.33\ \%$$

The previous equation and the X-ray diffractogram confirm that the powder sample indeed belongs to a CNC structure with a very high crystalline index above 80%.

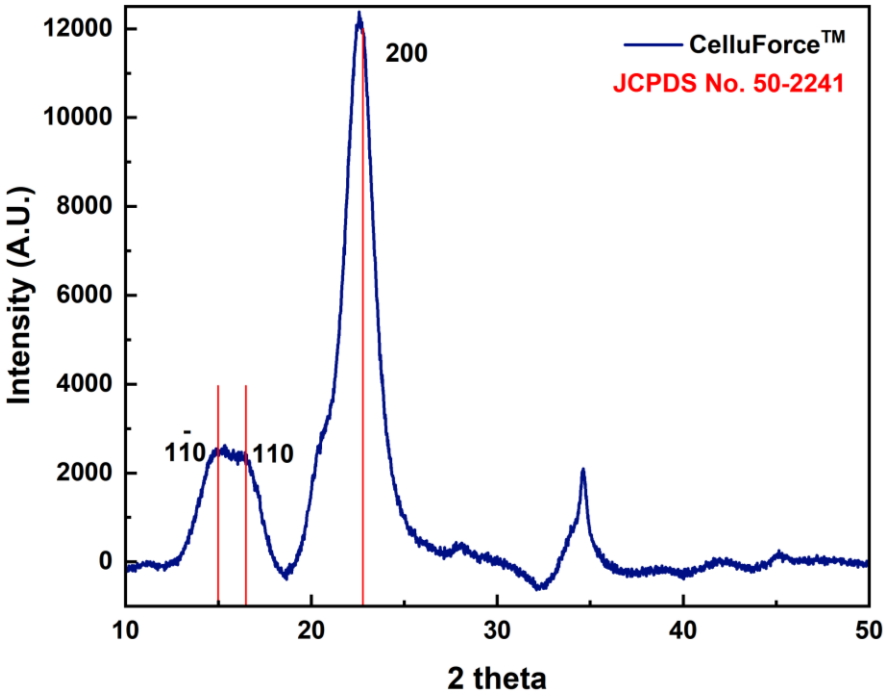

Figure 29. XRD pattern of the CNC. From CelluForce™

6.1.2 Functional groups quantification

|Described in the previous section, two different titrations were performed to calculate the sulfate half-esters (S-CNC) content as well as the carboxylic groups (COOH-CNC) on the CNC's surface. For both titrations, once the equivalence point was reached, the functional group's concentration was calculated using the following equation:

$$-OSO_3H/COOH = \frac{[NaOH]\, x\, Vol_{NaOH}}{m_{CNC}}$$

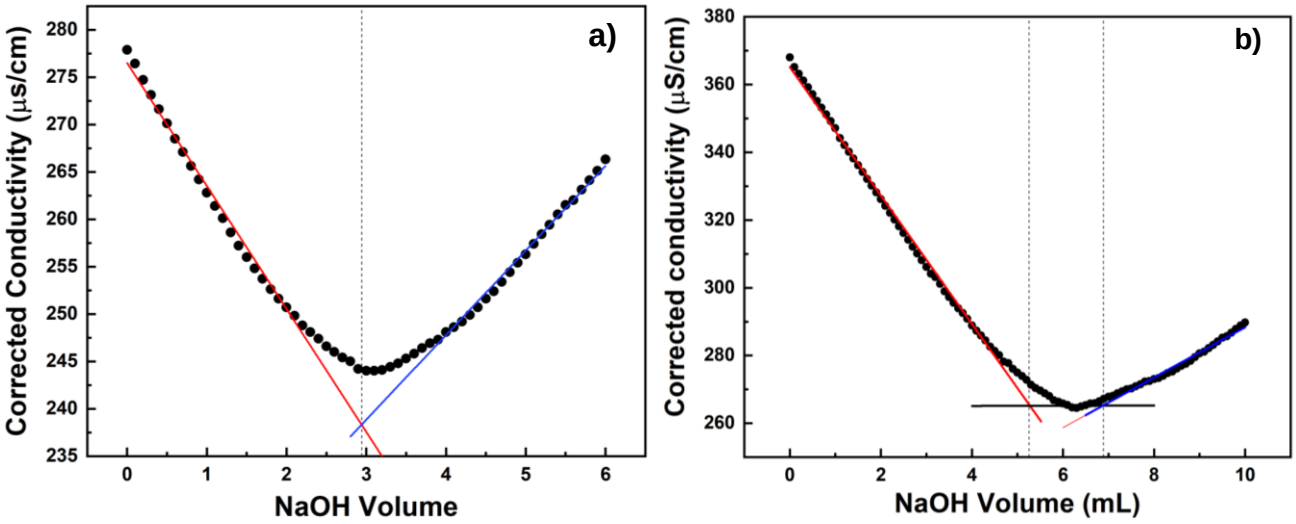

Figure 30. a) Conductometric titration curve of S-CNC titrated against NaOH (10 mM). b) Conductimetric titration curve of the COOH-CNC, same conditions.

Figure 30 shows the titration curves obtained for the both different CNCs (S-CNC and COOH-CNC). Red lines in the graphs represent the consumption of protons (neutralization) and the blue ones the excess of NaOH. For the case of strong acids titration (a), the typical graph shows a sharp transition at an early equivalence point, whereas the graph for the weak acids (b) a known concentration of strong acid is added to the suspension to establish a measurable reduction in conductivity at the beginning of the titration. The equivalence point in the weak acid plot is calculated from the volume difference $(V_2 - V_1)$ obtained from intersection of the plateau and the acidic and basic regions. Both graphs keep their corresponding shape according to literature, while the non-carboxylated CNC has only an equivalence point, the functionalized one has two points (for weak and strong acids, respectively) and the typical plateau, an indicator that the carboxylation was indeed achieved using a deep eutectic solvent composed of oxalic acid and choline chloride.

Presented in Table 3, the surface charge on the CNC's surface is presented in $mmol\ kg^{-1}$. As it can be observed, almost 0.3 $mmol\ g^{-1}$ of sulfate groups were calculated for the commercial CelluForce™'s CNC, similar to that reported in literature. [94]

Table 3 Quantification of functional groups before and after the carboxylation in DES.

Functional Group	Reaction time (h)	Weight (% to DES)	[ ] $mmol\ g^{-1}$
Sulfate groups (-OSO_3H)	-----	-----	0.3 ± 0.015
Carboxylic acids (-COOH)	3	5.0	0.2 ± 0.018

An FTIR spectra performed to the cellulose samples is presented in Figure 31. Typical peaks at 2900 cm^{-1} and 895 cm^{-1} are attributed to C-H stretching and β-glycosidic linkages of cellulose. On the contrary, a peak intensity at 1735 cm^{-1} is assigned to the carbonyl stretch of the carboxylic acid groups, whereas an increase in the band intensity at 1429 cm^{-1} is due to the $-COO^-$ symmetric stretching vibration [95], confirming the increase in the carboxylation of the CNC surface formed by the esterification reaction between the hydroxyl groups of cellulose and the carboxyl groups of the oxalic acid counterpart of the DES. The amount of carboxyl group content can be further confirmed by the band intensity at 1160, 1107, 1056 and 1030 cm^{-1} respectively assigned to the stretching and/or bending of -CO bond. [84] The measurement resolution used was 1 cm^{-1} and the spectra were collected in the range of 4000 – 400 cm^{-1}

Table 4 Peak intensities found in the different cellulose nanocrystals.

Peak intensity (cm^{-1})	*Bond*	*Reference.*
895, 2900	C-H stretching	[96]
1160	-CO stretching	[97]
1119, 1056	C-C stretching, -COC bending	[98]
1429	C-O bending	[99]
1735	-COO^- stretching	[100] [101]
3300	-OH stretching	[101]

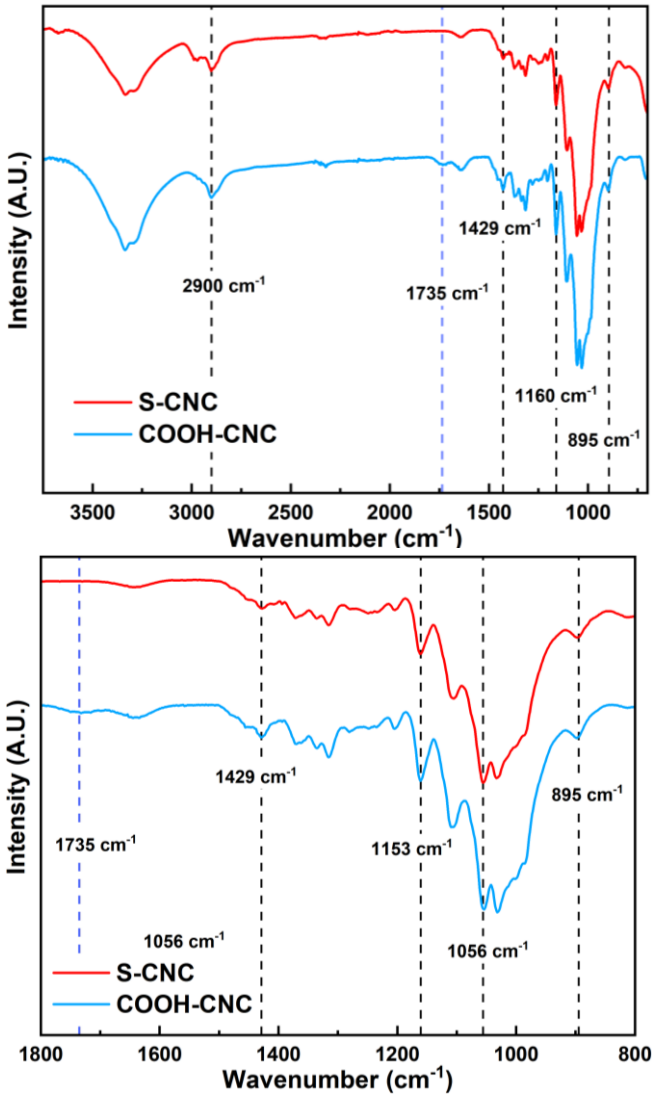

Figure 31. FTIR spectra of the commercial CNC (S-CNC) and the carboxylated CNC (COOH-CNC).

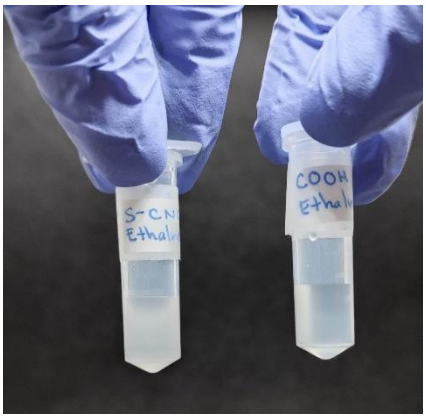

Figure 32. The carboxylated cellulose has a better dispersion in the ethaline DES (less turbid) compared to the S-CNC (1.0 wt% samples).

6.2 Eutectogels

By following the methodology described in section 5.2.2.5, different transparent, highly stretchable, non-volatile, viscous, and electrically conductive eutectogels were obtained with certain variations on its properties depending on the CNC content. For all the eutectogels, the DES liquid phase constitutes the vast majority of the eutectogel by volume and, because of its inherent composition comprising ionic species, the eutectogels also display an important ionic conductivity (~3.0 $mS\ cm^{-1}$). Compared to an aqueous solvent, the supramolecular structure of the eutectogels is characterized by a significant number of hydrogen bonds between its components (i.e., HBA and HBD), therefore, hydrogen bonding is the predominant non-covalent force responsible for the eutectogel's outstanding properties such as thermal stability, conductivity, stretchability, and optical properties that will be discussed in the next sections.

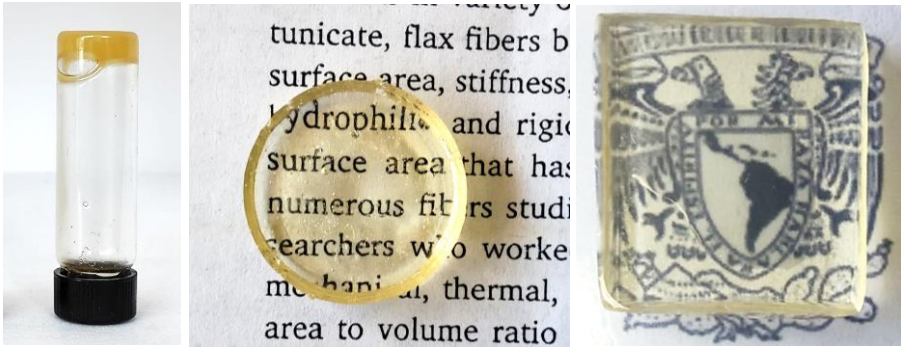

Figure 33. 22 wt% gelatin-based eutectogel prepared in a deep eutectic solvent.

The gel formation followed a bottom-up approach, where the inherent self-assembly strategy (double/triple helix formation) of the denatured collagen chains (gelatin) facilitates the gel formation and makes unnecessary the use of an additional chemical crosslinker agents. While the formation of a hydrogel it's also possible, the DES environment promotes a high number of non-covalent interactions due to solvophobic and hydrogen bonding interactions between the gelatin chains. Nonetheless, different types of non-covalent interactions (hydrogen bonding, hydrophobic and electrostatic interactions) may appear from the interplay between the DES components (ionic and non-ionic) and different functional groups on the denatured collagen chains such as amino, carboxylic and hydroxyl groups.

6.2.1 FTIR

To evaluate the changes in overall functional groups in the eutectogel compared with their precursors, i.e., gelatin and DES, the materials were studied by FTIR in the ATR mode. FTIR spectra revealed that the obtained eutectogel composites show similar characteristic peaks compared to its components (Figure 34). For the pure gelatin spectrum, the peaks at 1630, 1530, and 1450 cm^{-1} correspond to amide I (C=O), amide II (N-H) and carboxylic groups stretching, respectively, whereas the peak at 3300 corresponds to -OH vibrations. [102] In contrast to the neat DES, the eutectogel's spectra (without CNC) shares the aforementioned peaks due to the gelatin's presence in the gel matrix. In general, those peaks are more intense and slightly shifted to higher wavenumbers (1654, 1544 and 1481 cm^{-1}) possibly because of new interactions formed between the amide I and II groups, as well as the aminoacid's functional groups (carboxyl, hydroxyl etc.) and the solvent's counterparts, i.e, ethylene glycol and choline chloride.

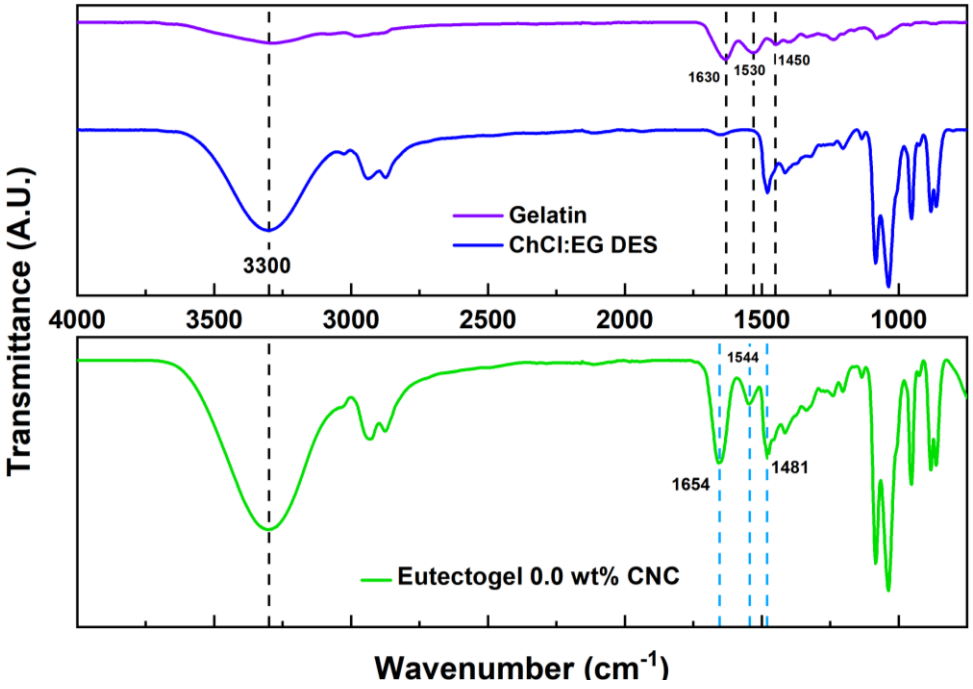

Figure 34. FTIR Spectra of DES, gelatin, and the non-reinforced eutectogel.

All those interactions formed between the DES and the gelatin are responsible for its high thermal stability and negligible loss in weight at room temperature due to volatility. Figure 35 depicts the stability in open conditions comparing the eutectogels and a hydrogel at room temperature. As can be seen, the low number of H-bonds in the hydrogel allows the water molecules to volatilize into the environment causing a continuous weight loss in the hydrogel. However, the H-bonding promoting structure of the DES and gelatin increases the material's life-span and therefore increases the material's practicality in a longer period of time.

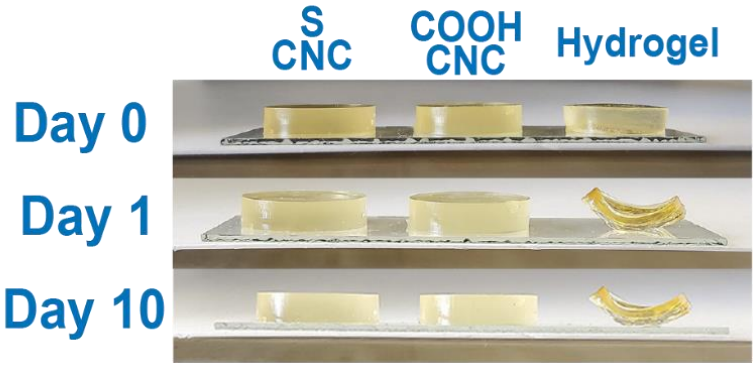

Figure 35. Weight loss is almost negligible for the eutectogels compared to a 22 wt% hydrogel.

The 1.0 wt% CNC reinforced eutectogels were also analyzed by FTIR to verify the new formed interactions of the CNC with the other eutectogel's components (Figure 36). For the S-CNC eutectogel, the FTIR seems to be quite similar to the neat eutectogel especially due to the fact that the DES spectra overlap the CNC's. Still, a slight increase in the bands at 1243 and 1197 cm^{-1} which belong to amide III groups is observed. [103]

On the other hand, the spectra of the carboxylated cellulose eutectogel is different compared to the others. As mentioned in section 6.1.2 the COOH-CNC has a characteristic peak in 1735 cm^{-1} which directly belongs to the carboxylic acids grafted in the nanocrystal's surface. Hence, the presence of the same peaks within the eutectogel has a shift towards a smaller wavenumber (1720 cm^{-1}) and implies the formation of new non-covalent interactions (possibly H-bonding) between the eutectogel components and the carboxylated cellulose, which could also be explained by an increase in the amide II band's intensity (1654 cm^{-1}). Also, the same increase of the bands at 1243 and 1197 cm^{-1} in the S-CNC occurs, an indicator of new interactions between the carboxylated CNC and the amide III groups. Lastly, the COOH-CNC resulted to be more

effective to promote the formation of new non-covalent interactions in the eutectogel, which is attributable to the abundance of hydrophilic groups in the material's surface.

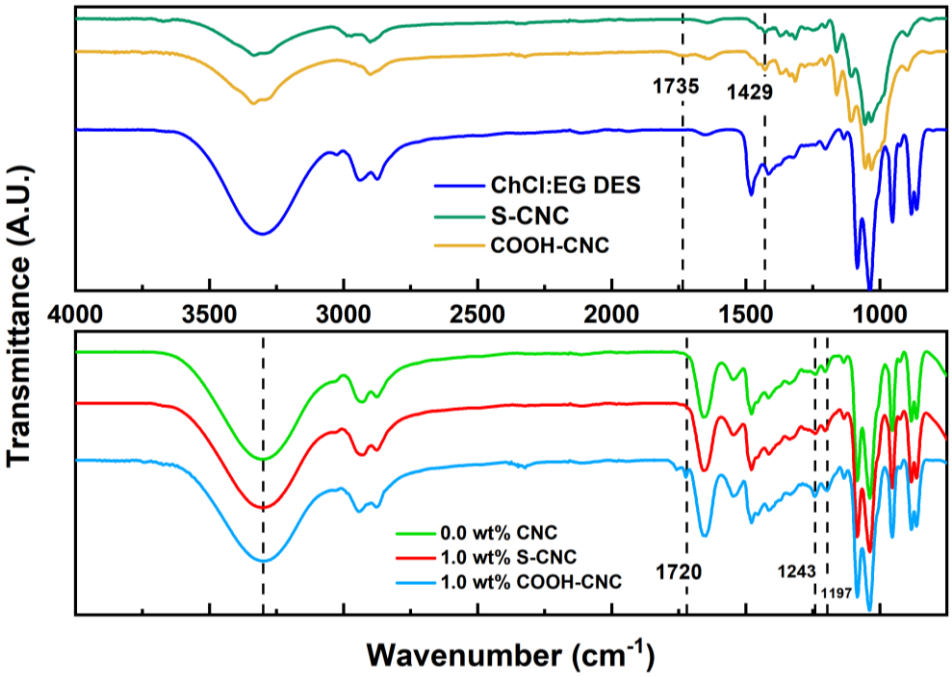

Figure 36. FTIR spectra of the different reinforced eutectogels.

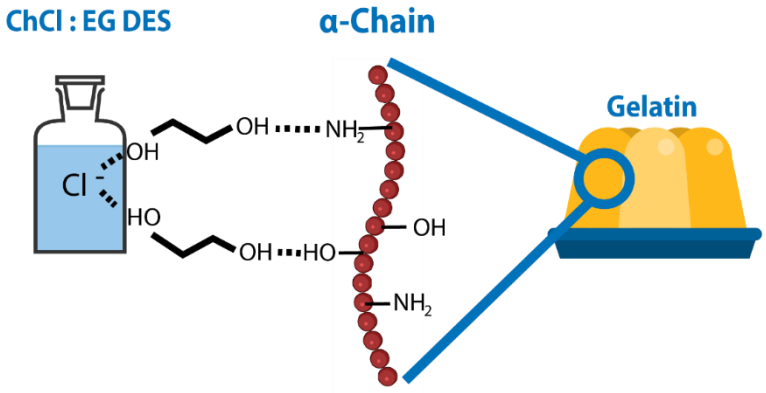

Figure 37. Schematic representation of the interactions formed between the gelatin and eutectogel. Contrary to a regular hydrogel, H bonds are abundant in a deep eutectic solvent, i.e., hydrogels do not present a remarkable performance. Image by author.

6.2.2 Transmittance measurements

Different gel samples were chosen to examine the transparency of the 22 wt% gelatin gels with different S-CNC and COOH-CNC content (0 - 1.0 wt%). According to Figure 38, the transparency of the eutectogels is clearly reduced as the cellulose content is increased in the eutectogel. While the eutectogel without CNC reaches a max transparency of ~94%, the 1.0 wt% S-CNC-containing eutectogel has the lowest transmittance of all the samples with ca. one third of the transmittance from the non-reinforced gel (~35%) associated with the scattering of the light and the difference between the diffraction index of both the eutectogel and the cellulose nanocrystals. However, the 1.0 wt% COOH-CNC gel barely reduced its transmittance compared to the S-CNC. This is explained by a better interface with the DES due to the abundance of carboxy groups on the COOH-CNC's surface which may be the responsible of a more homogenous dispersion in the solvent.

No matter the different degrees of transparency, the results certainly imply that the eutectogel's transparency can be tuned depending on the cellulose content, which is a useful strategy for the desired applications (sensing, optical light guide, etc.). Yet, the change in the transmittance is an indicator that the cellulose is integrated into the gel network.

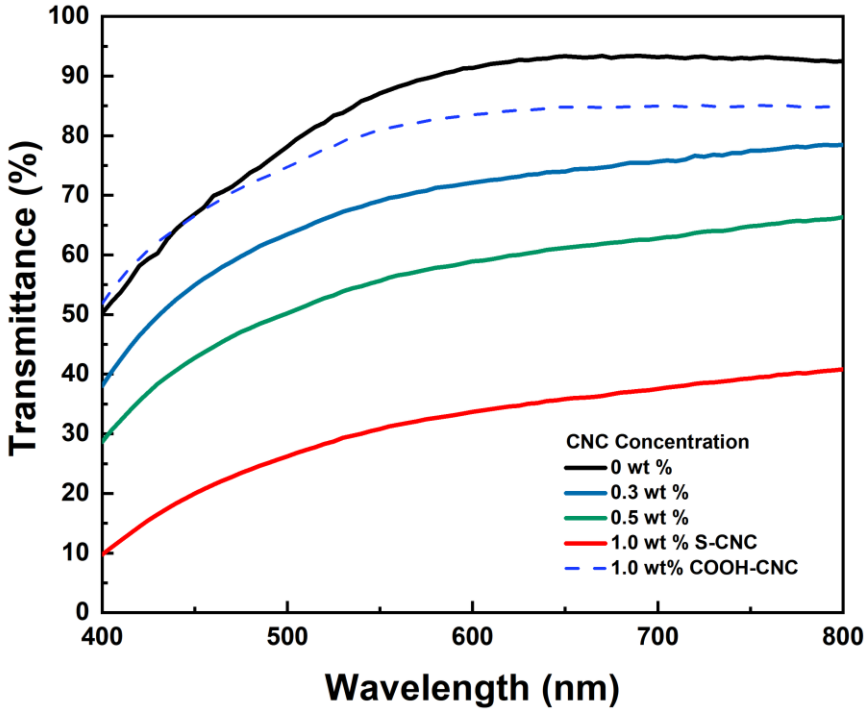

Figure 38. Transparency of the different eutectogels.

Figure 39. The reduction in transmittance is visually appreciable. (From left to right: 0, 0.3 0.5 and 1.0 wt% S-CNC.)

6.2.3 Birefringence phenomena

Birefringence is the optical property of a material that has a refractive index dependent on polarization and direction of the light. Hardly reported in the eutectogels' literature, a new birefringence effect is shown by the prepared CNC eutectogels. Figure 40 depicts different eutectogel samples under polarized light and a polarized filter, the figure shows how the birefringence effect is an excellent tool to visualize the nanocrystal's content in the different materials. As can be seen from the eutectogels (left), no optical effect is observed due to the absence of CNC, whereas the presence of the CNC clearly produces the notorious optical effect as the CNC content increases (0.3 to 1.0 wt% CNC).

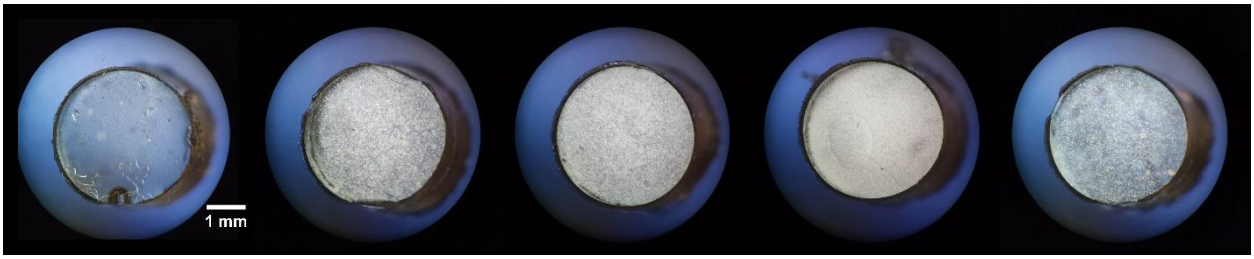

Figure 40. Eutectogels under a polarizer filter. (From left to right: 0.0, 0.3, 0.5 and 1.0 wt% S-CNC). At the right of the figure, 1.0 wt% COOH-CNC.

It is well known that in aqueous suspension, chiral nematic liquid crystalline phases appear only above a critical CNC concentration, however, as for the type of CNC composing the eutectogels, the birefringence here is associated with the structural anisotropy of the cellulose in the eutectogel [104] and, therefore, it's possible that the high heterogeneity of the S-CNC in the eutectogels promotes a more intense optical response compared to COOH-CNC at the same concentration, implying that a better dispersion (homogeneity) of the cellulose in the gelatin network is the responsible for reducing the intensity of the optical effect (promoting isotropic orientation).

Similar to liquid crystals, the alignment of the nanocrystals can change the polarization of transmitted light due to a phase difference, which can result in significant changes in interference color when viewed between crossed or parallel polarizers. [56] Actually, a prominent and interesting shear-induced birefringence phenomena is present in the eutectogels with the highest CNC concentrations (1.0 wt%). It is certainly possible that, while stretching the material, CNCs embedded in the eutectogel experienced a disordered to ordered transition, possibly in a preferential direction causing anisotropic birefringence along the material under polarized light (shown in Figure 42).

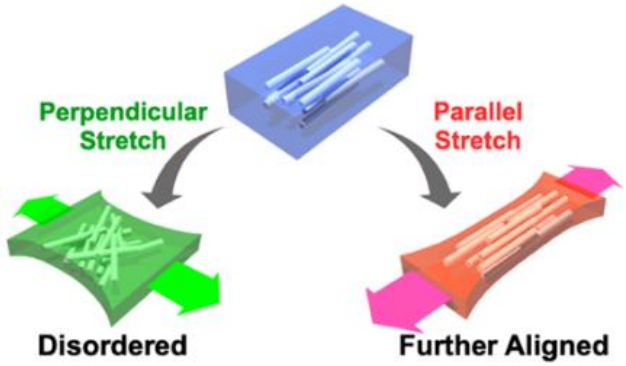

Figure 41. Schematic illustration of CNC reorientation in the composite. Macromolecules 2019, 52, 5317−5324.

Figure 42. Shear-birefringence effect shown by the 1.0 wt% S-CNC eutectogel under polarized light (Samsung Galaxy Tab S7). The effect intensifies as the material is stretched.

Hence, even if the material's transparency seems to be reduced by the CNC's addition, the reinforced eutectogels present a new mechano-optical effect with exciting applications in the optics field possibly as a double response sensor and 3D printing. Nonetheless, more measurements must be performed to explore the birefringence's potential such as rheology studies. Also, polarized

optical microscopy (POM) and optical probes can confirm the birefringence at different concentrations. [105] SEM/TEM have been used to directly observe the alignment of the nanocrystals, while polarized UV-Vis spectroscopy is capable of measuring the light transmittance by changing the orientation of the polarizers. [56]

6.2.4 Mechanical properties

6.2.4.1 Tensile tests

For the tensile tests, 23.64 mm length eutectogel probes with the highest CNC concentration (1.0 wt%) were used to evaluate their mechanical properties. As it was expected, the CNC in the eutectogel composites strongly influenced the material's performance. For the non-reinforced eutectogel previously reported, the ultimate average strain strength reached was 67 kPa and the maximum fracture strain occurred at ~300% of stretching, while the S-CNC eutectogel prepared in this work reached 60 kPa and a stretching of ~330%. Surprisingly, the COOH-CNC supports less stress (35 kPa) but its strain got boosted up to an average of ~375%.

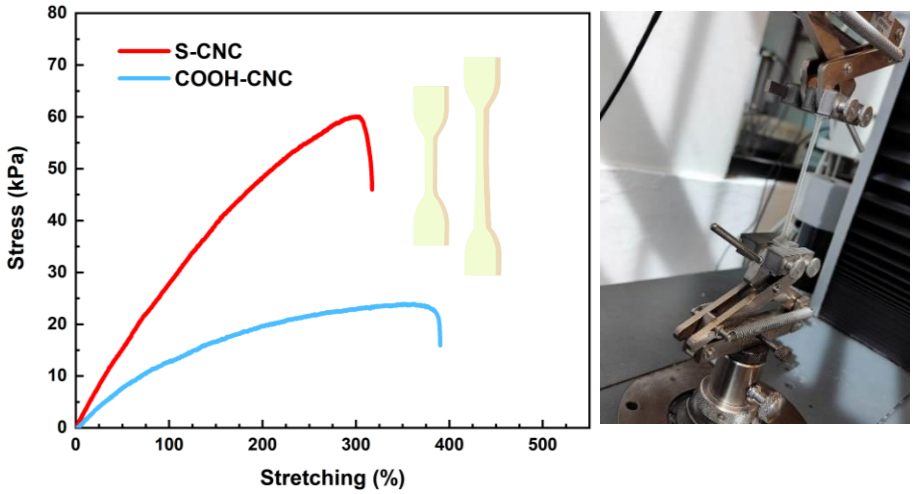

Figure 43. Representative tensile stress-strain curves for the 1.0 wt% CNC reinforced eutectogels.

Table 5 shows that the S-CNC's addition to the eutectogel barely reduces its Young's modulus compared to the eutectogel previously reported by the Panzer group. However, for the COOH-CNC there is a drop of about 50% compared to the non-reinforced gel. It's possible that due to the high carboxylic content in the CNC's surface, the number of hydrogen bonding and non-covalent interactions is higher that that in the commercial sulfated CNC, consequently, a strong interface is formed between the cellulose and the gelatin possibly reducing the triple helix formation

through those new interactions which partially block the three-dimensional network formation and, therefore, reducing the natural collagen's stiffness within the deep eutectic solvent. Nonetheless, the cellulose eutectogels show an acceptable ultimate tensile strength of 59 and 34 kPa for the S-CNC and COOH-CNC, respectively, which results higher than of some double network-based hydrogels reported in literature (4kPa). [106] Also, the new increase in stretchability (~374%) is higher than other gelatin-based materials used for soft robotics applications (~150%), [107] and close to other PVA/gelatin-based eutectogels (~400). [108]

Table 5. Mechanical properties extracted from the tensile test data for the eutectogels.

Eutectogel	Tensile strength **(kPa)**	Strain at break **(%)**	Young's Modulus **(kPa)**	Toughness **($kJ\ m^{-3}$)**	Reference
0 CNC	67	300	30	133	[89]
0 CNC	63	300 ± 22	30 ± 4	120 ± 12	This work
S-CNC	59	330 ± 12	26 ± 8	112 ± 11	This work
COOH-CNC	34	374 ± 23	15 ± 4	80 ± 19	This work

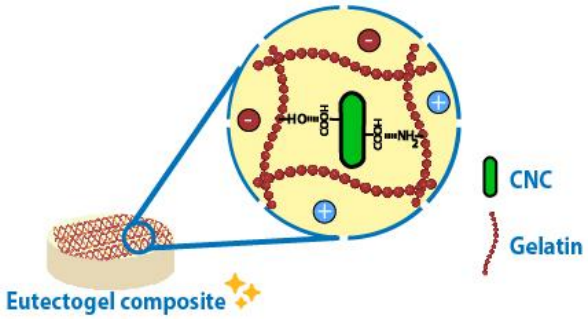

Figure 44. Possible non-covalent interactions formed through the COOH-CNC/Eutectogel composite. Image by author

Also, the low Young's modulus can be advantageously used for certain biomedical applications. The low stiffness in the composites enables a soft interaction with living tissues due to the fact that the Young's moduli of living tissues reported in literature range from 0.1 to 50000 kPa, [109] therefore the high stretching of the materials plus the softening of the material makes them suitable for the design of soft strain sensors.

6.2.4.2 Mechanical properties: Compressive tests

Figure 45 depicts a typical compressive stress-strain curve of the different eutectogels, where the samples were compressed up to 50% of its original height. From the hysteresis curves in the graph, is clearly visible that the materials could be compressed up to the max strain without any permanent shape change, where the gels used for the tests recover their original form immediately after releasing the pressure (inset). While the non-reinforced eutectogel reaches a max stress of ~90 kPa, the S-CNC and the COOH-CNC eutectogel reach a maximum value of 100 and 110 kPa respectively, representing an increase of 10% and 20% attributed to the cellulose addition in the eutectogel. Again, as discussed above, cellulose nanocrystals are likely the main responsible for the boost in the compressive properties due to the formation of new non-covalent interactions, which are present in a higher number in the COOH-CNC because the presence of carboxylic acids is conducive to form H-bonds through the gel network between the cellulose, gelatin and the DES itself, mainly in a nonaqueous environment.

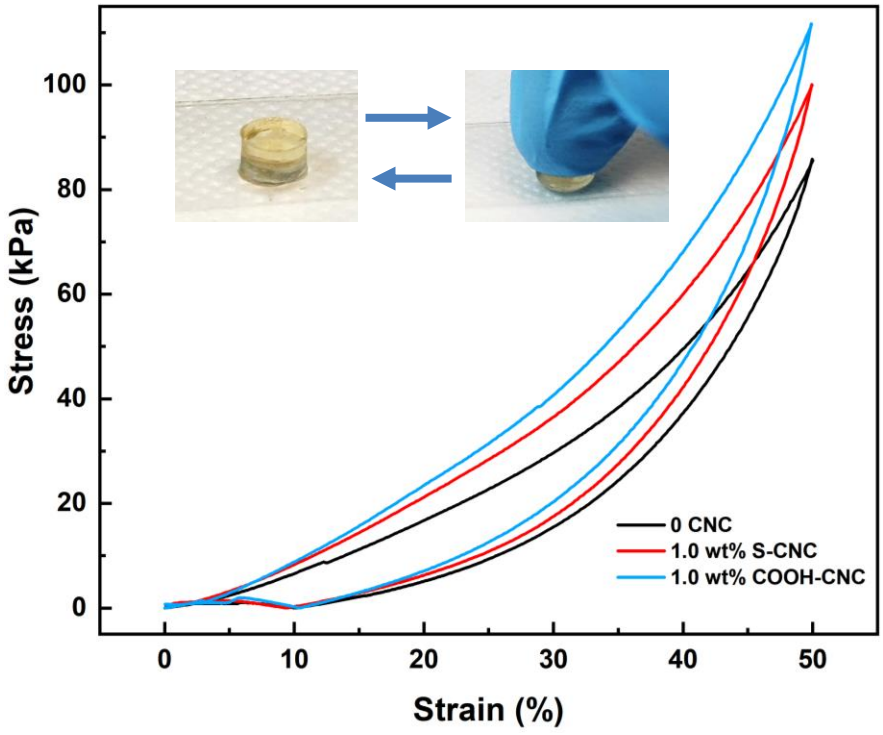

Figure 45. Compressive loading-unloading curve of the 1.0 wt% CNC eutectogels.

6.2.1 Ionic conductivity

The ionic conductivity of the gels was measured by EIS impedance spectroscopy at room temperature. Compared to ethaline's neat conductivity ($\sim$7.5 $mS\ cm^{-1}$), the pure eutectogel display a conductivity of $\sim$2.0 $mS\ cm^{-1}$, consequence of the changes in the DES hydrogen bond network caused by integration of gelatin ($\sim$22%). Also, the increase in the material's viscosity reduces the charge carrier's mobility in the material and therefore a decrease in the conductivity occurs.

To explore the gradual change in the conductivity as a function of the CNC content in the eutectogels, different concentrations of the nanomaterials were tested. As can be seen from the graph in Figure 46, there exists a tendency in the conductivity's increase that is directly proportional to the CNC addition. From the data in Table 6, it is observed that 0.5 wt% CNC added to the gels causes the conductivity to grow up to 50% of the original conductivity. However, once the highest concentration is added (1.0 wt%), the conductivity reaches a plateau. A possible explanation is that, while both CNCs are not conductive by themselves, the CNC's hygroscopic character could be responsible for retaining water from the environment and increasing the number of ionic species in the eutectogel after its addition. Based on the thermogram results of the DSC in Figure 49 only thermal events related to the gelatin-CNC occur whereas water-related events are negligible in the eutectogels. Therefore, it is possible that what causes the increase in conductivity is the presence of not free water but bound and non-freezing water in the network. [110]

Table 6. Ionic conductivities obtained for different CNC composites.

CNC (wt %)	S-CNC Conductivity ($\mathrm{mS\ cm^{-1}}$)	COOH-CNC Conductivity ($\mathrm{mS\ cm^{-1}}$)
0.0	2.0 ± 0.06	
0.1	2.6 ± 0.1	2.8 ± 0.2
0.5	3.1 ± 0.2	3.0 ± 0.1
1.0	3.0 ± 0.13	2.9 ± 0.1

Different electronic circuits were designed to test the conductivity of the eutectogels in a simple fashion. As can be seen from both Figure 47 and Figure 48, the eutectogels are capable of conducting electricity through daily life electronic devices, which is a desired property in the soft materials and flexible electronics area for the design of flexible and non-conventional circuits.

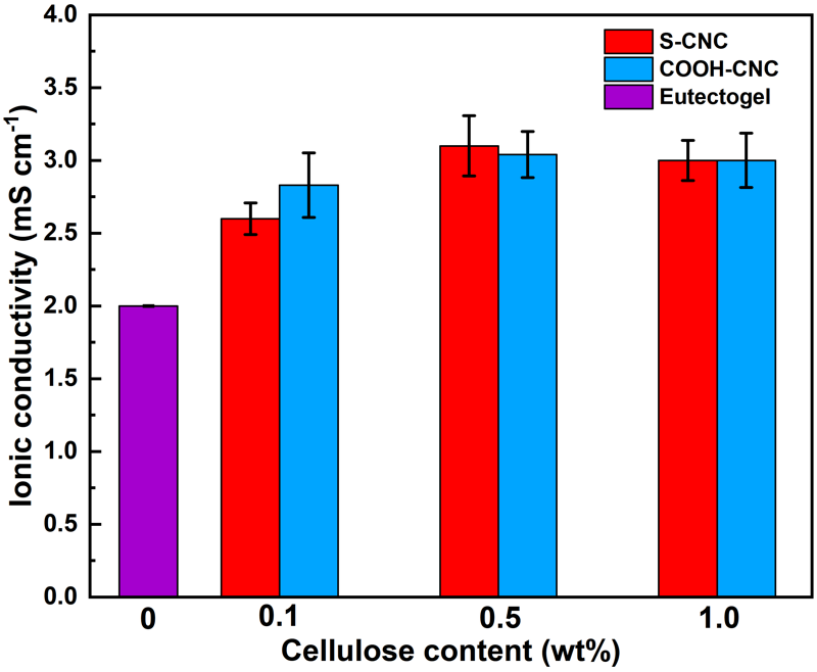

Figure 46. Conductivity results from the ionic measurements using the EIS technique.

Finally, the ionic conductivity of 3.0 $mS\ cm^{-1}$ exhibited by the eutectogels thanks to CNC addition is an outstanding result. According to literature, the obtained value is higher than other flexible materials based on gelatin and/or deep eutectic solvents. Previously reported, Fan et al. designed a highly stretchable polymer based on PVI/MBA in a ChCl:Gly DES [111], whereas the Zhang group prepared a PVA based polymer [112] with conductivities of 1.54 and 0.35 $mS\ cm^{-1}$ at room temperature, respectively. Also, gelatin based eutectogels prepared in a reline DES [108] and an acrylic acid eutectogel prepared in an ethaline DES [113] achieved 1.37 and 1.26 $mS\ cm^{-1}$, respectively, i.e., well below the values obtained in this work.

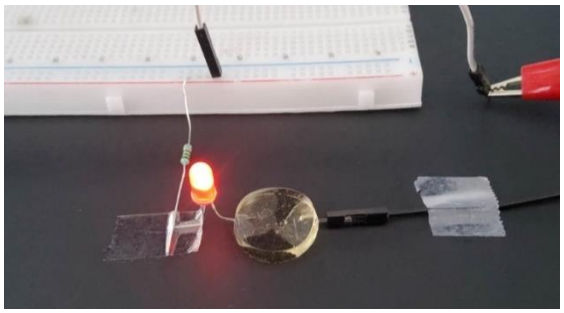

Figure 47. Eutectogels can conduct electricity due to their high content of ionic species.

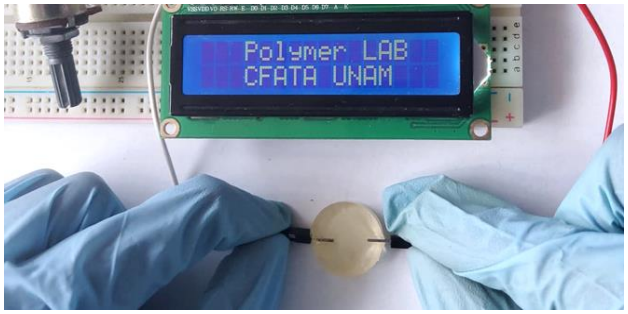

Figure 48. Eutectogel's conductivity is enough to display a 16x2 LCD. Image by author.

6.2.2 DSC (Differential scanning calorimetry)

DSC is a thermoanalytical technique that measures the energy transferred to or from a sample undergoing a chemical or physical change as a function of temperature. Thermographs in Figure 49 describe the presence of thermal event during the heating run. As can be seen, neat DES remains stable under the range of temperate from 0 to 140 °C (the reported Tg of ethaline is -116 °C by DSC), whereas different melting points appear in the materials due to the polymeric counterpart, e.g, gelatin, and gelatin-CNC complex. For the eutectogel without CNC, a melting point occurs at 38 °C and is attributed to the gelatin melting in the DES, which in contrast with the melting point observed in water with concentration of 25wt. %, which is ca. 43 °C. [114] However, for the CNC-based eutectogels the semi-solid to liquid transition measured as endothermic events, have a slight shift towards higher temperatures which is caused by the effective interactions between CNC and gelatin promoted by the DES. The FTIR spectra described in section 6.2.1 shows evidence of the formation of new non-covalent interactions along the gel networks and, hence, more energy is required to break those non-covalent interactions increasing the thermal stability of the materials.

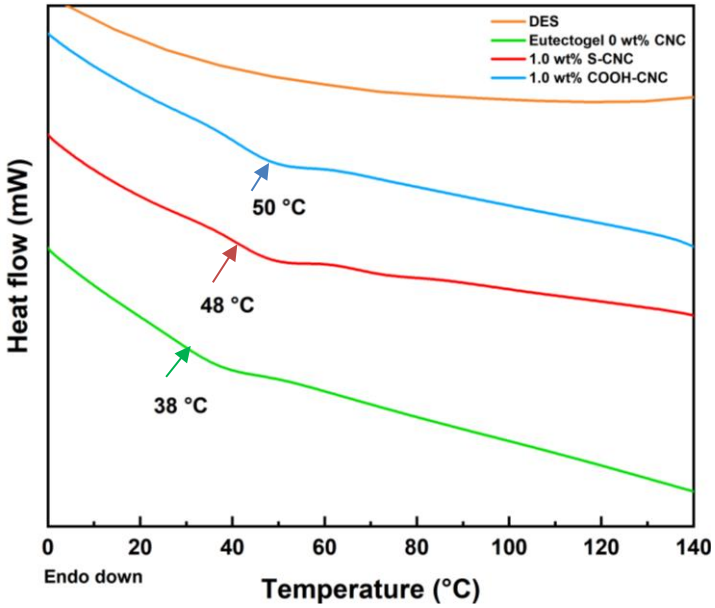

Figure 49. DSC Thermographs of the different eutectogels varying the CNC composition.

As expected, the cellulose's addition to the gels increased the thermal stability of the gels. From the previous graph, it's evident that the carboxylated CNC has a slight shift of 2 °C for the

gelatin melting point attributed to a higher number of H-bonds and a strong interface between CNC with gelatin and the DES. However, this change was not reflected in the eutectogels practical performance as the softening of the gels still begins at temperatures close to human's body ($\sim 40\,°C$). Despite the thermal stability limits the material's potential as wearable devices or applications with higher temperature requirements, it opens the path for their use under low temperatures and even vacuum. [111] [115] [116]

On the other hand, the thermal properties of the eutectogels can be advantageously used to explore the self-healing effect after heating and melting a previously used sample ($\sim 50\,°C$) and then recasting it into a mold. Thanks to its non-covalent bonds, the eutectogels can be fully recycled after used only by heating the samples at considerable low temperatures, which don't' represent a high energetic cost to reuse the gels. It is worthy to mention that, even if the material reaches its maximum recyclability capacity, the material can be indeed disposed without any extra purification storage, or treatment because of the intrinsically biodegradable character of all its components: cellulose, gelatin, ethylene glycol and choline chloride.

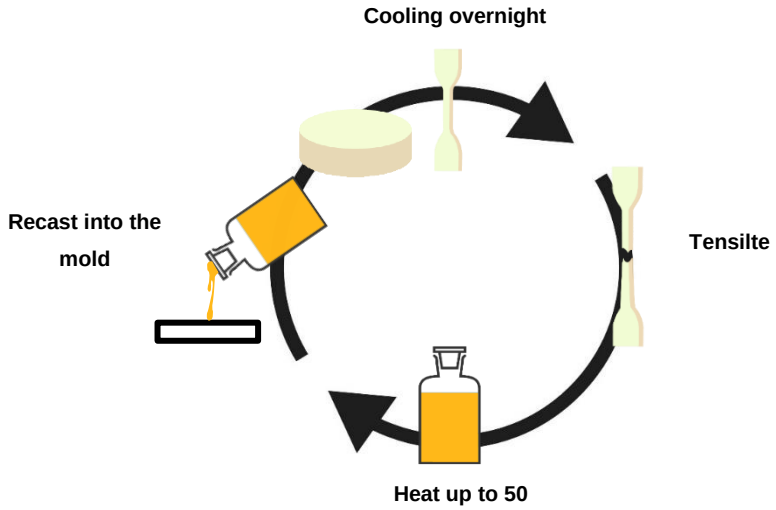

Figure 50. Recyclability of the eutectogels

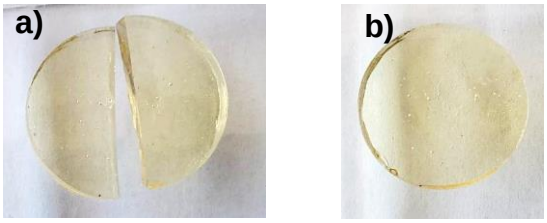

Figure 51. Self-healing displayed by the eutectogels. a) Sample before being heated up to 50 °C. b) Gel after being casted and cooled again at 4 °C overnight.

6.2.3 Wearable strain-sensor design

To demonstrate the material's potential as a stimuli-responsive material in curved surfaces, a strain sensor was fabricated as a wearable device in an extended finger by using a rectangular piece (4 x 23.64 mm) of the prepared eutectogels; cupper tape was used for electrical connections on the edges of the eutectogels. After the connections were set, the strain-sensitive eutectogel was fixed onto the joint of a finger where different tensile deformations were applied to the eutectogels by varying the bending angle causing a change in the resistance. All the measurements were conducted by using a digital Multimeter (Sparkfun Electronic 70C) kindly donated by Dr. Nicolas R. Tanguy. Using intervals of time of 20 seconds, different tensile deformations were applied in angles ranging from 0 to 120° causing a systematically increase (and decrease) in the resistance.

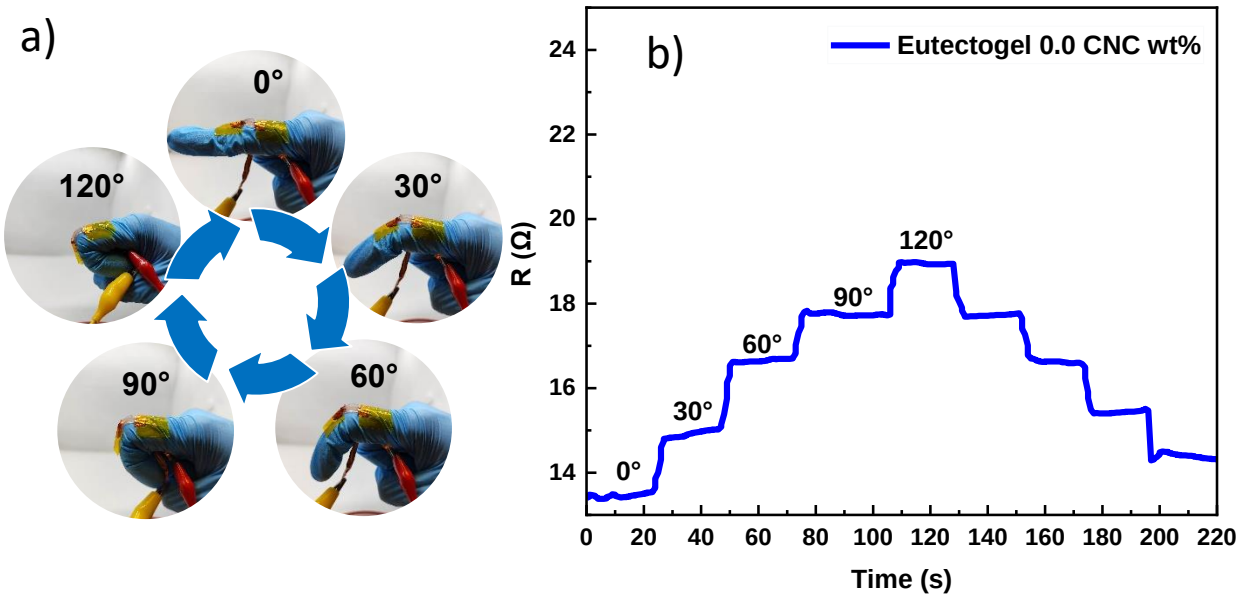

Figure 52. a) Tensile deformations applied to the eutectogels. b) Demonstration of the change in resistance of the eutectogel as a wearable sensor.

In the compressive tests in Figure 45, the hysteresis curve demonstrates that the material could be compressed without suffering any permanent damage and is capable of recovering its original shape. This phenomenon is quite useful to describe Figure 52, where the hysteresis shown by the eutectogels explains why the same change in the resistance is obtained once the material is returned to its original position. In summary, these results demonstrate that the prepared eutectogels exhibit an outstanding response in real-time as well as a high sensibility and an excellent recovery in shape as well as in conductivity terms.

A useful parameter to evaluate the strains sensitivity of a sensor is the gauge factor (GF), which is defined as the slope of the plot of relative resistance versus an applied strain. [117] The GF is calculated by using the following equation:

$$\frac{\Delta R}{\Delta L} = \frac{\frac{R - R_0}{R_0}}{\frac{L - L_0}{L_0}}$$

Where R is the resistance and L is the length of the sample. The GFs of the 3 different eutectogels were calculated at room temperature by stretching the materials up to 100% of its original length. A GF of 1.3 was calculated for the non-reinforced eutectogel, whereas a GF of 1.5 and 2.3 was calculated for the S-CNC gel and the COOH-CNC gel, respectively. This increment in the GF could be attributed not only to the increase of the ionic conductivity due to the CNC's presence, but also by the reduction in the Young's modulus, which means that less strain is necessary to promote a deformation in the material.

7. Conclusions

In the present work, gelatin based eutectogels with different cellulose nanocrystals content homogeneously integrated within the gel were prepared. The influence of the CNC surface chemistry (sulfated or carboxylated) on the overall physicochemical and mechanical properties of the eutectogels was studied. The results clearly show a positive effect in the material's mechanical, electrical and thermal properties compared to the non-reinforced eutectogels, specially for the carboxylated CNC due to its higher performance. Different concentrations of CNC were tested, up to 1 wt.% dispersed in the DES suspension precursor and ultimately homogeneously integrated within the eutectogel network. COOH-CNC having carboxylic groups at the surface promoted a higher number of non-covalent interactions with gelatin and the DES, enhancing the stretchability, the ionic conductivity, the thermal stability and promoting a birefringence effect. Thus, addition of the biobased nanomaterials such as CNC in different proportions opens the path to selectively tune the eutectogels properties depending on the desired applications such as light guide, strain sensors, substrate for flexible electronics, actuators and more.

In summary:

1. The functionalization of the CNC in the oxalic acid-choline chloride (1:1 molar ratio) DES pose a sustainable means to modify the surface chemistry of commercial sulfated CNC.

According to the FTIR spectra, it was identified the presence of new carboxylic acid's characteristic peaks. The characteristic curve for the titration of weak acids (COOH) also confirms the presence of those groups on the surface obtaining $\sim 0.2\, mmol\, g^{-1}$ of carboxylic groups, which is similar to values obtained with TEMPO and other conventional methods of oxidation. [54] [61] [65] [66]

2. The transparency of the eutectogels can be tuned by varying the concentration of CNC. An unprecedent optical effect of shear-induced birefringence is displayed by the CNC composites that did not exist in the previously reported pure eutectogels.
3. While the S-CNC has a modest increased in the mechanical properties in the eutectogels, the COOH-CNC increased the stretching in almost 75%. However, there exist a decreasing in the material's stiffness and toughness.
4. Remarkably, CNC's addition led to an increase of ionic conductivity. The water content and overall ionic and non-covalent interactions within the eutectogels network led to an increased conductivity up to $\sim 3.0\, mS\, cm^{-1}$, higher than some other gelatin and DES-based materials and hydrogels reported in the literature [118]:

Table 7. Properties of eutectogels based on different DES and polymers composition.

Eutectogel	Tensile Strain (%)	$\sigma\ (mS\, cm^{-1})$	GF
Gelatin/Ethaline	300	2.5	0.5
Starch/Glycine	300	/	0.55
WPU/Glycine	395	0.22	2.15
DBS/Reline	/	0.2	/
MXene/AM/AA DES (3 ChCl:4 Urea)	1750	0.0015	/
Gellan Gum/(ChCl:HEA)/Reline	1835	0.41	1.18
Gelatin S-CNC/Ethaline (This work)	330	3.0	1.5
Gelatin COOH-CNC/Ethaline (This work)	375	3.0	2.3

5. The cellulose addition increased the melting points of the eutectogels in a maximum of 12 °C for the COOH-CNC. Yet, the low melting points allows the materials to be fully recyclable through heating and recasting the material into a mold.

8. Future perspectives

The current research sets a new direction for the preparation of greener soft materials. From what can be seen from Table 7, the results obtained from this research clearly demonstrate that the designed materials have a high performance in terms of conductivity, sensitivity (GF) and mechanical properties compared to works that have been previously reported. While the incorporation of other cellulosic nanomaterials remains unexplored, in order to extend the full potential of biodegradable gelatin and cellulose based eutectogels, some points to remark are as follows:

- In order to promove a higher number of non-covalent interactions between the cellulose, gelatin and DES, cellulose nanocrystals can be further functionalized to increase the number of carboxylic acids through a different molar relation of the oxalic acid DES. [66]
- A recent and novel approach to increase the number of crosslinks in the gelatin is the treatment with tannic acid. Exploiting the physical crosslinking with multifunctional biobased molecules may promote more interactions between the gelatin, the solvent and the cellulose. [119] [120]
- Instead of functionalizing the surface with carboxylic groups through covalent bonds, it has been reported that cellulose nanocrystals may be coated with tannic acid or phytic to improve mechanical and viscoelastic properties of hydrogels to promote H-bonding with a polymer matrix. [121]
- Gelatin methacrylate (GelIMA) has been used as an alternative to conventional gelatin for the design of e-skinks and hydrogels. [122]
- Some authors have been reported that the mechanical reinforcement of the CNCs is often limitated by their aggregation. Adding a polymeric additive to the gels may be a good alternative to disperse the cellulose and to promote stronger interactions in the materials. [123]
- Replacing the gelatin for more thermostable biopolymers it’s a good alternative. Xantham gum has been proposed as a gel matrix with good thermal properties even at higher temperatures like 80 °C, making it a good candidate for a wearable soft material. [88]

9. References

[1] D. Corzo, G. Tostado-Blázquez, and D. Baran, “Flexible Electronics: Status, Challenges and Opportunities,” *Front. Electron.*, vol. 1, no. September, pp. 1–13, 2020, doi: 10.3389/felec.2020.594003.

[2] National Resarch Council, *The Flexible Electronics Opportunity*. Washington, DC: The National Academies Press, 2014.

[3] L. Zhang *et al.*, “Overview of Ionogels in Flexible Electronics,” *Chem. Rec.*, vol. 20, no. 9, pp. 948–967, 2020, doi: 10.1002/tcr.202000041.

[4] R. Das, X. He, and G. K, “Flexible, Printed and Organic Electronics 2020-2030: Forecasts, Technologies, Markets,” 2020.

[5] V. K. Khanna, *Flexible Electronics*, vol. 3. 2019.

[6] W. Gao, H. Ota, D. Kiriya, K. Takei, and A. Javey, “Flexible Electronics toward Wearable Sensing,” *Acc. Chem. Res.*, vol. 52, no. 3, pp. 523–533, 2019, doi: 10.1021/acs.accounts.8b00500.

[7] Z. Zhou, H. Zhang, J. Liu, and W. Huang, “Flexible electronics from intrinsically soft materials,” *Giant*, vol. 6, p. 100051, 2021, doi: 10.1016/j.giant.2021.100051.

[8] P. Wang *et al.*, “The Evolution of Flexible Electronics: From Nature, Beyond Nature, and To Nature,” *Adv. Sci.*, vol. 7, no. 20, pp. 1–29, 2020, doi: 10.1002/advs.202001116.

[9] M. Sala de Medeiros, D. Chanci, and R. V. Martinez, “Moisture-insensitive, self-powered paper-based flexible electronics,” *Nano Energy*, vol. 78, no. June, p. 105301, 2020, doi: 10.1016/j.nanoen.2020.105301.

[10] J. D. Mota-Morales and E. Morales-Narváez, “Transforming nature into the next generation of bio-based flexible devices: New avenues using deep eutectic systems,” *Matter*, vol. 4, no. 7, pp. 2141–2162, 2021, doi: 10.1016/j.matt.2021.05.009.

[11] C. Seife, “The Runners-Up,” *Science (80-.).*, 2000.

[12] C. Majidi, “Soft-Matter Engineering for Soft Robotics,” *Adv. Mater. Technol.*, vol. 4, no. 2, pp. 1–13, 2019, doi: 10.1002/admt.201800477.

[13] A. Fernandez-Nieves and A. M. Puertas, *Fluids, Colloids and Soft Materials: An Introduction to Soft Matter Physics*. 2018.

[14] J. L. Drury and D. J. Mooney, “Hydrogels for tissue engineering: Scaffold design variables and applications,” *Biomaterials*, vol. 24, no. 24, pp. 4337–4351, 2003, doi: 10.1016/S0142-9612(03)00340-5.

[15] P. E. Dupont *et al.*, “A decade retrospective of medical robotics research from 2010 to 2020,” *Sci. Robot.*, vol. 6, no. 60, 2021, doi: 10.1126/scirobotics.abi8017.

[16] L. C. Tomé and D. Mecerreyes, “Emerging Ionic Soft Materials Based on Deep Eutectic Solvents,” *J. Phys. Chem. B*, vol. 124, no. 39, pp. 8465–8478, 2020, doi: 10.1021/acs.jpcb.0c04769.

[17] H. R. Lee, C. C. Kim, and J. Y. Sun, “Stretchable Ionics – A Promising Candidate for Upcoming Wearable Devices,” *Adv. Mater.*, vol. 30, no. 42, pp. 1–15, 2018, doi: 10.1002/adma.201704403.

[18] M. J. Panzer, “Holding it together: noncovalent cross-linking strategies for ionogels and eutectogels,” *Materials Advances*. Royal Society of Chemistry, 2022, doi: 10.1039/d2ma00539e.

[19] H. C. Ates *et al.*, “End-to-end design of wearable sensors,” *Nat. Rev. Mater.*, vol. 15, no. 2, pp. 1–23, 2022, doi: 10.1038/s41578-022-00460-x.

[20] S. Petros, T. Tesfaye, and M. Ayele, “A Review on Gelatin Based Hydrogels for Medical Textile Applications,” *J. Eng. (United Kingdom)*, vol. 2020, 2020, doi: 10.1155/2020/8866582.

[21] Y. Lee, W. J. Song, and J. Y. Sun, “Hydrogel soft robotics,” *Mater. Today Phys.*, vol. 15, p. 100258, 2020, doi: 10.1016/j.mtphys.2020.100258.

[22] M. Guo *et al.*, “A highly stretchable, ultra-tough, remarkably tolerant, and robust self-healing glycerol-hydrogel for a dual-responsive soft actuator,” *J. Mater. Chem. A*, vol. 7, no. 45, pp. 25969–25977, 2019, doi: 10.1039/C9TA10183G.

[23] S. Lin *et al.*, “Stretchable Hydrogel Electronics and Devices,” *Adv. Mater.*, vol. 28, no. 22, pp. 4497–4505, Jun. 2016, doi: https://doi.org/10.1002/adma.201504152.

[24] Y. Zhang, M. Gong, and P. Wan, “MXene hydrogel for wearable electronics,” *Matter*, vol. 4, no. 8, pp. 2655–2658, 2021, doi: 10.1016/j.matt.2021.06.041.

[25] O. S. Hammond and A. V. Mudring, “Ionic liquids and deep eutectics as a transformative platform for the synthesis of nanomaterials,” *Chem. Commun.*, vol. 58, no. 24, pp. 3865–3892, 2022, doi: 10.1039/d1cc06543b.

[26] Q. Zhang, K. De Oliveira Vigier, S. Royer, and F. Jérôme, “Deep eutectic solvents: Syntheses, properties and applications,” *Chem. Soc. Rev.*, vol. 41, no. 21, pp. 7108–7146, 2012, doi: 10.1039/c2cs35178a.

[27] R. Tamate *et al.*, “Self-Healing Micellar Ion Gels Based on Multiple Hydrogen Bonding,” *Adv. Mater.*, vol. 30, no. 36, p. 1802792, Sep. 2018, doi: https://doi.org/10.1002/adma.201802792.

[28] G. García, S. Aparicio, R. Ullah, and M. Atilhan, “Deep eutectic solvents: Physicochemical properties and gas separation applications,” *Energy and Fuels*, vol. 29, no. 4, pp. 2616–2644, 2015, doi: 10.1021/ef5028873.

[29] M. Francisco, A. van den Bruinhorst, and M. C. Kroon, “Low-transition-temperature mixtures (LTTMs): a new generation of designer solvents.,” *Angew. Chem. Int. Ed. Engl.*, vol. 52, no. 11, pp. 3074–3085, Mar. 2013, doi: 10.1002/anie.201207548.

[30] Y. Zhang *et al.*, “Methods for fabrication of flexible hybrid electronics,” no. August 2017, p. 12, 2017, doi: 10.1117/12.2275561.

[31] X. H. Yang and W. L. Zhu, “Viscosity properties of sodium carboxymethylcellulose solutions,” *Cellulose*, vol. 14, no. 5, pp. 409–417, 2007, doi: 10.1007/s10570-007-9137-9.

[32] T. Ghosh, R. Deveswaran, and S. Bharath, “Copper crosslinked carboxymethyl chitosan–gelatin scaffolds: A potential antibacterial and cytocompatible material for biomedical applications,” *Mater. Today Proc.*, vol. 59, pp. 31–38, 2022, doi: 10.1016/j.matpr.2021.10.140.

[33] J. Alipal *et al.*, “A review of gelatin: Properties, sources, process, applications, and

commercialisation," *Mater. Today Proc.*, vol. 42, pp. 240–250, 2019, doi: 10.1016/j.matpr.2020.12.922.

[34] T. R. Keenan, "Gelatin," *Polym. Sci. A Compr. Ref. 10 Vol. Set*, vol. 10, pp. 237–247, 2012, doi: 10.1016/B978-0-444-53349-4.00265-X.

[35] L.-C. Lv, Q.-Y. Huang, W. Ding, X.-H. Xiao, H.-Y. Zhang, and L.-X. Xiong, "Fish gelatin: The novel potential applications," *J. Funct. Foods*, vol. 63, p. 103581, 2019, doi: https://doi.org/10.1016/j.jff.2019.103581.

[36] S. Sultana, M. E. Ali, and M. N. U. Ahamad, "11 - Gelatine, collagen, and single cell proteins as a natural and newly emerging food ingredients," in *Woodhead Publishing Series in Food Science, Technology and Nutrition*, M. E. Ali and N. N. A. B. T.-P. and P. of R. and C. F. Nizar, Eds. Woodhead Publishing, 2018, pp. 215–239.

[37] Z. A. Nur Hanani, Y. H. Roos, and J. P. Kerry, "Use and application of gelatin as potential biodegradable packaging materials for food products," *Int. J. Biol. Macromol.*, vol. 71, pp. 94–102, 2014, doi: https://doi.org/10.1016/j.ijbiomac.2014.04.027.

[38] P. J. Flory and E. S. Weaver, "Helix [UNK] Coil Transitions in Dilute Aqueous Collagen Solutions1," *J. Am. Chem. Soc.*, vol. 82, no. 17, pp. 4518–4525, Sep. 1960, doi: 10.1021/ja01502a018.

[39] J. Calvarro, T. Perez-Palacios, and J. Ruiz, "Modification of gelatin functionality for culinary applications by using transglutaminase," *Int. J. Gastron. Food Sci.*, vol. 5–6, pp. 27–32, 2016, doi: https://doi.org/10.1016/j.ijgfs.2016.11.001.

[40] Y. Zeng *et al.*, "Preformed gelatin microcryogels as injectable cell carriers for enhanced skin wound healing," *Acta Biomater.*, vol. 25, pp. 291–303, 2015, doi: https://doi.org/10.1016/j.actbio.2015.07.042.

[41] K. Ma, X. Cai, Y. Zhou, Y. Wang, and T. Jiang, "In Vitro and In Vivo Evaluation of Tetracycline Loaded Chitosan-Gelatin Nanosphere Coatings for Titanium Surface Functionalization," *Macromol. Biosci.*, vol. 17, no. 2, p. 1600130, Feb. 2017, doi: https://doi.org/10.1002/mabi.201600130.

[42] M. Baumgartner *et al.*, "Resilient yet entirely degradable gelatin-based biogels for soft robots

and electronics," *Nat. Mater.*, vol. 19, no. 10, pp. 1102–1109, 2020, doi: 10.1038/s41563-020-0699-3.

[43] S. Edward and H. M. Golecki, "Gelatin Soft Actuators: Benefits and Opportunities," *Actuators*, vol. 12, no. 2, 2023, doi: 10.3390/act12020063.

[44] T. Nagai, A. Kurita, and J. Shintake, "Characterization of Sustainable Robotic Materials and Finite Element Analysis of Soft Actuators Under Biodegradation," *Front. Robot. AI*, vol. 8, 2021, doi: 10.3389/frobt.2021.760485.

[45] H. Harris *et al.*, "Development and Characterization of Biostable Hydrogel Robotic Actuators for Implantable Devices: Tendon Actuated Gelatin." Apr. 11, 2022, doi: 10.1115/DMD2022-1049.

[46] D. Trache *et al.*, *Nanocellulose: From Fundamentals to Advanced Applications*, vol. 8, no. May. 2020.

[47] A. Dufresne, "Nanocellulose: A new ageless bionanomaterial," *Mater. Today*, vol. 16, no. 6, pp. 220–227, 2013, doi: 10.1016/j.mattod.2013.06.004.

[48] J. Tang, J. Sisler, N. Grishkewich, and K. C. Tam, "Functionalization of cellulose nanocrystals for advanced applications," *J. Colloid Interface Sci.*, vol. 494, pp. 397–409, 2017, doi: 10.1016/j.jcis.2017.01.077.

[49] P. Mali and A. P. Sherje, "Cellulose nanocrystals: Fundamentals and biomedical applications," *Carbohydr. Polym.*, vol. 275, no. August 2021, p. 118668, 2022, doi: 10.1016/j.carbpol.2021.118668.

[50] H. Kargarzadeh *et al.*, *Advances in cellulose nanomaterials*, vol. 25, no. 4. Springer Netherlands, 2018.

[51] K. Köse, M. Mavlan, and J. P. Youngblood, "Applications and impact of nanocellulose based adsorbents," *Cellulose*, vol. 27, no. 6, pp. 2967–2990, 2020, doi: 10.1007/s10570-020-03011-1.

[52] B. Thomas *et al.*, "Nanocellulose, a Versatile Green Platform: From Biosources to Materials and Their Applications," *Chem. Rev.*, vol. 118, no. 24, pp. 11575–11625, 2018, doi: 10.1021/acs.chemrev.7b00627.

[53] R. J. Moon, G. T. Schueneman, and J. Simonsen, “Overview of Cellulose Nanomaterials, Their Capabilities and Applications,” *Jom*, vol. 68, no. 9, pp. 2383–2394, 2016, doi: 10.1007/s11837-016-2018-7.

[54] J. A. Sirviö, M. Visanko, and H. Liimatainen, “Acidic Deep Eutectic Solvents As Hydrolytic Media for Cellulose Nanocrystal Production,” *Biomacromolecules*, vol. 17, no. 9, pp. 3025–3032, 2016, doi: 10.1021/acs.biomac.6b00910.

[55] Y. Habibi, “Key advances in the chemical modification of nanocelluloses,” *Chem. Soc. Rev.*, vol. 43, no. 5, pp. 1519–1542, 2014, doi: 10.1039/c3cs60204d.

[56] O. Kose, C. E. Boott, W. Y. Hamad, and M. J. Maclachlan, “Stimuli-Responsive Anisotropic Materials Based on Unidirectional Organization of Cellulose Nanocrystals in an Elastomer,” *Macromolecules*, vol. 52, no. 14, pp. 5317–5324, 2019, doi: 10.1021/acs.macromol.9b00863.

[57] J. H. Jordan, M. W. Easson, and B. D. Condon, “Alkali hydrolysis of sulfated cellulose nanocrystals: Optimization of reaction conditions and tailored surface charge,” *Nanomaterials*, vol. 9, no. 9, 2019, doi: 10.3390/nano9091232.

[58] D. Zhalmuratova and H. J. Chung, “Reinforced Gels and Elastomers for Biomedical and Soft Robotics Applications,” *ACS Appl. Polym. Mater.*, vol. 2, no. 3, pp. 1073–1091, 2020, doi: 10.1021/acsapm.9b01078.

[59] Z. Zhang, G. Sèbe, D. Rentsch, T. Zimmermann, and P. Tingaut, “Ultralightweight and flexible silylated nanocellulose sponges for the selective removal of oil from water,” *Chem. Mater.*, vol. 26, no. 8, pp. 2659–2668, 2014, doi: 10.1021/cm5004164.

[60] N. S. Çetin *et al.*, “Acetylation of cellulose nanowhiskers with vinyl acetate under moderate conditions,” *Macromol. Biosci.*, vol. 9, no. 10, pp. 997–1003, 2009, doi: 10.1002/mabi.200900073.

[61] E. Lam and U. D. Hemraz, “Preparation and surface functionalization of carboxylated cellulose nanocrystals,” *Nanomaterials*, vol. 11, no. 7, 2021, doi: 10.3390/nano11071641.

[62] Y. Chen, J. Zhu, H. Y. Yu, and Y. Li, “Fabricating robust soft-hard network of self-healable polyvinyl alcohol composite films with functionalized cellulose nanocrystals,” *Compos. Sci.*

Technol., vol. 194, no. March, p. 108165, 2020, doi: 10.1016/j.compscitech.2020.108165.

[63] L. Cao, W. Liu, and L. Wang, “Developing a green and edible film from Cassia gum: The effects of glycerol and sorbitol,” *J. Clean. Prod.*, vol. 175, pp. 276–282, 2018, doi: 10.1016/j.jclepro.2017.12.064.

[64] Y. Habibi, L. A. Lucia, and O. J. Rojas, “Cellulose Nanocrystals: Chemistry, Self-Assembly, and Applications.,” *Chem. Rev.*, vol. 110, pp. 3479–3500, 2010.

[65] K. J. Haunreiter, A. B. Dichiara, and R. Gustafson, “Nanocellulose by Ammonium Persulfate Oxidation: An Alternative to TEMPO-Mediated Oxidation,” *ACS Sustain. Chem. Eng.*, vol. 10, no. 12, pp. 3882–3891, Mar. 2022, doi: 10.1021/acssuschemeng.1c07814.

[66] X. Cao, M. Liu, W. Bi, J. Lin, and D. D. Y. Chen, “Direct carboxylation of cellulose in deep eutectic solvent and its adsorption behavior of methylene blue,” *Carbohydr. Polym. Technol. Appl.*, vol. 4, no. May, p. 100222, 2022, doi: 10.1016/j.carpta.2022.100222.

[67] A. P. Abbott, G. Capper, D. L. Davies, R. K. Rasheed, and V. Tambyrajah, “Novel solvent properties of choline chloride/urea mixtures,” *Chem. Commun.*, no. 1, pp. 70–71, 2003, doi: 10.1039/b210714g.

[68] E. L. Smith, A. P. Abbott, and K. S. Ryder, “Deep Eutectic Solvents (DESs) and Their Applications,” *Chem. Rev.*, vol. 114, no. 21, pp. 11060–11082, 2014, doi: 10.1021/cr300162p.

[69] L. I. N. Tomé, V. Baião, W. da Silva, and C. M. A. Brett, “Deep eutectic solvents for the production and application of new materials,” *Appl. Mater. Today*, vol. 10, pp. 30–50, 2018, doi: 10.1016/j.apmt.2017.11.005.

[70] T. El Achkar, H. Greige-Gerges, and S. Fourmentin, “Basics and properties of deep eutectic solvents: a review,” *Environ. Chem. Lett.*, vol. 19, no. 4, pp. 3397–3408, 2021, doi: 10.1007/s10311-021-01225-8.

[71] J. García-Álvarez, “Deep Eutectic Mixtures: Promising Sustainable Solvents for Metal-Catalysed and Metal-Mediated Organic Reactions,” *Eur. J. Inorg. Chem.*, vol. 2015, no. 31, pp. 5147–5157, 2015, doi: 10.1002/ejic.201500892.

[72] Y. P. Mbous, M. Hayyan, A. Hayyan, W. F. Wong, M. A. Hashim, and C. Y. Looi, “Applications

of deep eutectic solvents in biotechnology and bioengineering—Promises and challenges," *Biotechnol. Adv.*, vol. 35, no. 2, pp. 105–134, 2017, doi: 10.1016/j.biotechadv.2016.11.006.

[73] A. P. Abbott, D. Boothby, G. Capper, D. L. Davies, and R. K. Rasheed, "Deep Eutectic Solvents Formed between Choline Chloride and Carboxylic Acids : Versatile Alternatives to Ionic Liquids," no. 9, pp. 9142–9147, 2004.

[74] A. P. Abbott, D. Boothby, G. Capper, D. L. Davies, and R. K. Rasheed, "Deep Eutectic Solvents Formed between Choline Chloride and Carboxylic Acids: Versatile Alternatives to Ionic Liquids," *J. Am. Chem. Soc.*, vol. 126, no. 29, pp. 9142–9147, Jul. 2004, doi: 10.1021/ja048266j.

[75] G. R. T. Jenkin *et al.*, "The application of deep eutectic solvent ionic liquids for environmentally-friendly dissolution and recovery of precious metals," *Miner. Eng.*, vol. 87, pp. 18–24, 2016, doi: https://doi.org/10.1016/j.mineng.2015.09.026.

[76] A. P. Abbott, K. S. Ryder, and U. König, "Electrofinishing of metals using eutectic based ionic liquids," *Trans. IMF*, vol. 86, no. 4, pp. 196–204, Jul. 2008, doi: 10.1179/174591908X327590.

[77] F. S. Oliveira, A. B. Pereiro, L. P. N. Rebelo, and I. M. Marrucho, "Deep eutectic solvents as extraction media for azeotropic mixtures," *Green Chem.*, vol. 15, no. 5, pp. 1326–1330, 2013, doi: 10.1039/C3GC37030E.

[78] D. Di Marino, M. Shalaby, S. Kriescher, and M. Wessling, "Corrosion of metal electrodes in deep eutectic solvents," *Electrochem. commun.*, vol. 90, pp. 101–105, 2018, doi: https://doi.org/10.1016/j.elecom.2018.04.011.

[79] C. Lu, J. Cao, N. Wang, and E. Su, "Significantly improving the solubility of non-steroidal anti-inflammatory drugs in deep eutectic solvents for potential non-aqueous liquid administration," *Medchemcomm*, vol. 7, no. 5, pp. 955–959, 2016, doi: 10.1039/C5MD00551E.

[80] S. Kumar-Krishnan *et al.*, "Temperature-induced Au nanostructure synthesis in a nonaqueous deep-eutectic solvent for high performance electrocatalysis," *J. Mater. Chem. A*, vol. 3, no. 31, pp. 15869–15875, 2015, doi: 10.1039/c5ta02606g.

[81] C. Gu and J. Tu, “One-Step Fabrication of Nanostructured Ni Film with Lotus Effect from Deep Eutectic Solvent,” *Langmuir*, vol. 27, no. 16, pp. 10132–10140, Aug. 2011, doi: 10.1021/la200778a.

[82] R. P. Swatloski, S. K. Spear, J. D. Holbrey, and R. D. Rogers, “Dissolution of cellose with ionic liquids,” *J. Am. Chem. Soc.*, vol. 124, no. 18, pp. 4974–4975, 2002, doi: 10.1021/ja025790m.

[83] H. Zhang, J. Lang, P. Lan, H. Yang, J. Lu, and Z. Wang, “Study on the dissolution mechanism of cellulose by ChCl-based deep eutectic solvents,” *Materials (Basel).*, vol. 13, no. 2, pp. 1–12, 2020, doi: 10.3390/ma13020278.

[84] Z. Ling *et al.*, “Structural variations of cotton cellulose nanocrystals from deep eutectic solvent treatment: micro and nano scale,” *Cellulose*, vol. 26, no. 2, pp. 861–876, 2019, doi: 10.1007/s10570-018-2092-9.

[85] B. Joos, T. Vranken, W. Marchal, M. Safari, M. K. Van Bael, and A. T. Hardy, “Eutectogels: A New Class of Solid Composite Electrolytes for Li/Li-Ion Batteries,” *Chem. Mater.*, vol. 30, no. 3, pp. 655–662, 2018, doi: 10.1021/acs.chemmater.7b03736.

[86] M. Mokhtarpour, H. Shekaari, and A. Shayanfar, “Design and characterization of ascorbic acid based therapeutic deep eutectic solvent as a new ion-gel for delivery of sunitinib malate,” *J. Drug Deliv. Sci. Technol.*, vol. 56, p. 101512, 2020, doi: https://doi.org/10.1016/j.jddst.2020.101512.

[87] L. Zheng, H. Hua, Z. Zhang, Y. Zhu, L. Wang, and Y. Li, “PVA/ChCl Deep Eutectic Polymer Blends for Transparent Strain Sensors with Antifreeze, Flexible, and Recyclable Properties,” *ACS Appl. Mater. Interfaces*, 2022, doi: 10.1021/acsami.2c15673.

[88] C. Zeng, H. Zhao, Z. Wan, Q. Xiao, H. Xia, and S. Guo, “Highly biodegradable, thermostable eutectogels prepared by gelation of natural deep eutectic solvents using xanthan gum: preparation and characterization,” *RSC Adv.*, vol. 10, no. 47, pp. 28376–28382, 2020, doi: 10.1039/d0ra03390a.

[89] H. Qin, R. E. Owyeung, S. R. Sonkusale, and M. J. Panzer, “Highly stretchable and nonvolatile gelatin-supported deep eutectic solvent gel electrolyte-based ionic skins for strain and pressure sensing,” *J. Mater. Chem. C*, vol. 7, no. 3, pp. 601–608, 2019, doi:

10.1039/c8tc05918g.

[90] V. Vatanpour, A. Dehqan, and A. R. Harifi-Mood, “Ethaline deep eutectic solvent as a hydrophilic additive in modification of polyethersulfone membrane for antifouling and separation improvement,” *J. Memb. Sci.*, vol. 614, no. July, p. 118528, 2020, doi: 10.1016/j.memsci.2020.118528.

[91] E. J. Foster *et al.*, “Current characterization methods for cellulose nanomaterials,” *Chem. Soc. Rev.*, vol. 47, no. 8, pp. 2609–2679, 2018, doi: 10.1039/c6cs00895j.

[92] R. E. Owyeung, S. R. Sonkusale, and M. J. Panzer, “Influence of Hydrogen Bond Donor Identity and Intentional Water Addition on the Properties of Gelatin-Supported Deep Eutectic Solvent Gels,” *J. Phys. Chem. B*, vol. 124, no. 28, pp. 5986–5992, 2020, doi: 10.1021/acs.jpcb.0c03361.

[93] J. Gong, J. Li, J. Xu, Z. Xiang, and L. Mo, “Research on cellulose nanocrystals produced from cellulose sources with various polymorphs,” *RSC Adv.*, vol. 7, no. 53, pp. 33486–33493, 2017, doi: 10.1039/c7ra06222b.

[94] M. V. Kiriakou, A. S. Pakdel, R. M. Berry, T. Hoare, M. A. Dubé, and E. D. Cranston, “Incorporation of Polymer-Grafted Cellulose Nanocrystals into Latex-Based Pressure-Sensitive Adhesives,” *ACS Mater. Au*, 2021, doi: 10.1021/acsmaterialsau.1c00052.

[95] Z. Ling *et al.*, “Structural variations of cotton cellulose nanocrystals from deep eutectic solvent treatment: micro and nano scale,” *Cellulose*, vol. 26, no. 2, pp. 861–876, 2019, doi: 10.1007/s10570-018-2092-9.

[96] C. M. Lee, X. Chen, P. A. Weiss, L. Jensen, and S. H. Kim, “Quantum Mechanical Calculations of Vibrational Sum-Frequency-Generation (SFG) Spectra of Cellulose: Dependence of the CH and OH Peak Intensity on the Polarity of Cellulose Chains within the SFG Coherence Domain,” *J. Phys. Chem. Lett.*, vol. 8, no. 1, pp. 55–60, 2017, doi: 10.1021/acs.jpclett.6b02624.

[97] R. G. Zhbankov, S. P. Firsov, D. K. Buslov, N. A. Nikonenko, M. K. Marchewka, and H. Ratajczak, “Structural physico-chemistry of cellulose macromolecules. Vibrational spectra and structure of cellulose,” *J. Mol. Struct.*, vol. 614, no. 1–3, pp. 117–125, 2002, doi: 10.1016/S0022-2860(02)00252-1.

[98] J. J. Cael, J. L. Koening, and J. Blackwell, “Infrared and raman spectroscopy of carbohydrates part 4. Identification of configuration- and conformation-sensitive modes for D-glucose by normal coordinate analysis,” *Carbohydr. Res.*, vol. 32, pp. 79–91, 1974.

[99] M. F. Rosa *et al.*, “Cellulose nanowhiskers from coconut husk fibers: Effect of preparation conditions on their thermal and morphological behavior,” *Carbohydr. Polym.*, vol. 81, no. 1, pp. 83–92, 2010, doi: 10.1016/j.carbpol.2010.01.059.

[100] L. T. Cuba-Chiem, L. Huynh, J. Ralston, and D. A. Beattie, “In situ particle film ATR FTIR spectroscopy of carboxymethyl cellulose adsorption on talc: Binding mechanism, pH effects, and adsorption kinetics,” *Langmuir*, vol. 24, no. 15, pp. 8036–8044, 2008, doi: 10.1021/la800490t.

[101] G. Socrates, *Infrared and Raman characteristic group frequencies. Tables and charts*. 2001.

[102] R. Jiabing, H. Jingxiao, C. Li, S. Xinyu, and T. Hua, “Preparation and Characterization of Gelatin/ Hydroxyapatite Nanocomposite for Bone Tissue Engineering,” *Polym. Polym. Compos.*, vol. 38, no. 8, 2015, doi: 10.1002/pc.

[103] M. P. Das, S. P. R., K. Prasad, V. Jv, and R. M, “EXTRACTION AND CHARACTERIZATION OF GELATIN: A FUNCTIONAL BIOPOLYMER,” *Int. J. Pharm. Pharm. Sci.*, vol. 9, no. 9, pp. 239–242, 2017, doi: 10.22159/ijpps.2017v9i9.17618.

[104] A. A. Moud, M. Kamkar, A. Sanati-Nezhad, and S. H. Hejazi, *Suspensions and hydrogels of cellulose nanocrystals (CNCs): characterization using microscopy and rheology*, vol. 29, no. 7. Springer Netherlands, 2022.

[105] V. Hynninen *et al.*, “Inverse Thermoreversible Mechanical Stiffening and Birefringence in a Methylcellulose/Cellulose Nanocrystal Hydrogel,” *Biomacromolecules*, vol. 19, no. 7, pp. 2795–2804, 2018, doi: 10.1021/acs.biomac.8b00392.

[106] I. Jeon, J. Cui, W. R. K. Illeperuma, J. Aizenberg, and J. J. Vlassak, “Extremely Stretchable and Fast Self-Healing Hydrogels,” *Adv. Mater.*, vol. 28, no. 23, pp. 4678–4683, Jun. 2016, doi: https://doi.org/10.1002/adma.201600480.

[107] J. Shintake, H. Sonar, E. Piskarev, J. Paik, and D. Floreano, “Soft pneumatic gelatin actuator for edible robotics,” in *2017 IEEE/RSJ International Conference on Intelligent Robots and*

Systems (IROS), 2017, pp. 6221–6226, doi: 10.1109/IROS.2017.8206525.

[108] T. Chen, X. Mai, L. Ma, Z. Li, J. Wang, and S. Yang, “Poly(vinyl alcohol)/Gelatin-Based Eutectogels for the Sensitive Strain Sensor with Recyclability and Multienvironmental Suitability,” *ACS Appl. Polym. Mater.*, 2022, doi: 10.1021/acsapm.2c00425.

[109] A. C. Patil, Z. Xiong, and N. V Thakor, “Toward Nontransient Silk Bioelectronics: Engineering Silk Fibroin for Bionic Links,” *Small Methods*, vol. 4, no. 10, p. 2000274, Oct. 2020, doi: https://doi.org/10.1002/smtd.202000274.

[110] L. Solhi *et al.*, “Understanding Nanocellulose-Water Interactions: Turning a Detriment into an Asset,” *Chem. Rev.*, vol. 123, no. 5, pp. 1925–2015, 2023, doi: 10.1021/acs.chemrev.2c00611.

[111] K. Fan *et al.*, “Highly Stretchable, Self-Healing, and Adhesive Polymeric Eutectogel Enabled by Hydrogen-Bond Networks for Wearable Strain Sensor,” *SSRN Electron. J.*, vol. 449, no. April, p. 137878, 2022, doi: 10.2139/ssrn.4092246.

[112] H. Zhang, N. Tang, X. Yu, M. Li, and J. Hu, “Strong and Tough Physical Eutectogels Regulated by the Spatiotemporal Expression of Non-Covalent Interactions,” vol. 2206305, pp. 1–10, 2022, doi: 10.1002/adfm.202206305.

[113] G. Li *et al.*, “A stretchable and adhesive ionic conductor based on polyacrylic acid and deep eutectic solvents,” *npj Flex. Electron.*, vol. 5, no. 1, pp. 1–8, 2021, doi: 10.1038/s41528-021-00118-8.

[114] B. A. Harley, J. H. Leung, E. C. C. M. Silva, and L. J. Gibson, “Mechanical characterization of collagen-glycosaminoglycan scaffolds,” *Acta Biomater.*, vol. 3, no. 4, pp. 463–474, 2007, doi: 10.1016/j.actbio.2006.12.009.

[115] Y. Wu, Y. Deng, K. Zhang, J. Qiu, J. Wu, and L. Yan, “Ultrahigh Conductive and Stretchable Eutectogel Electrolyte for High-Voltage Flexible Antifreeze Quasi-solid-state Zinc-Ion Hybrid Supercapacitor,” *ACS Appl. Energy Mater.*, vol. 5, no. 3, pp. 3013–3021, Mar. 2022, doi: 10.1021/acsaem.1c03654.

[116] Y. Zhang, Y. Wang, Y. Guan, and Y. Zhang, “Peptide-enhanced tough, resilient and adhesive eutectogels for highly reliable strain/pressure sensing under extreme conditions.,” *Nat.*

Commun., vol. 13, no. 1, p. 6671, Nov. 2022, doi: 10.1038/s41467-022-34522-z.

[117] D. Wang *et al.*, “A strong, ultrastretchable, antifreezing and high sensitive strain sensor based on ionic conductive fiber reinforced organohydrogel,” *Compos. Part B Eng.*, vol. 243, no. April, p. 110116, 2022, doi: 10.1016/j.compositesb.2022.110116.

[118] Y. Gao *et al.*, “Highly Stretchable, Self-Healable and Self-Adhesive Double-Network Eutectogel Based on Gellan Gum and Polymerizable Deep Eutectic Solvent for Strain Sensing,” *ChemistrySelect*, vol. 8, no. 12, 2023, doi: 10.1002/slct.202204463.

[119] J. Piella, N. G. Bastús, and V. Puntes, “Size-Controlled Synthesis of Sub-10-nanometer Citrate-Stabilized Gold Nanoparticles and Related Optical Properties.,” *Chem. Mater.*, vol. 28, no. 4, pp. 1066–1075, 2016, doi: 10.1021/acs.chemmater.5b04406.

[120] J. Wang, F. Tang, Y. Wang, Q. Lu, S. Liu, and L. Li, “Self-Healing and Highly Stretchable Gelatin Hydrogel for Self-Powered Strain Sensor,” *ACS Appl. Mater. Interfaces*, vol. 12, no. 1, pp. 1558–1566, 2020, doi: 10.1021/acsami.9b18646.

[121] A. Carnicero *et al.*, “Ascidian-Inspired Supramolecular Cellulose Nanocomposite Hydrogels with Antibacterial Activity,” *ACS Biomater. Sci. Eng.*, vol. 8, no. 11, pp. 5027–5037, 2022, doi: 10.1021/acsbiomaterials.2c00935.

[122] B. Liu *et al.*, “Hydrogen bonds autonomously powered gelatin methacrylate hydrogels with super-elasticity, self-heal and underwater self-adhesion for sutureless skin and stomach surgery and E-skin,” *Biomaterials*, vol. 171, pp. 83–96, 2018, doi: 10.1016/j.biomaterials.2018.04.023.

[123] W. Meesorn, A. Shirole, D. Vanhecke, L. M. De Espinosa, and C. Weder, “A Simple and Versatile Strategy to Improve the Mechanical Properties of Polymer Nanocomposites with Cellulose Nanocrystals,” *Macromolecules*, vol. 50, no. 6, pp. 2364–2374, 2017, doi: 10.1021/acs.macromol.6b02629.